Chronic states of iron deficiency and excess in combination with erastin: An *in-vitro* study of acute monocytic leukemia (THP-1 cells).

By

Zachariah A. H. Fenniri

A Thesis Submitted in Partial Fulfillment
of the Requirements for the Degree of

BACHELOR OF SCIENCE (HONS.)

Department of Biology, Faculty of Science
University of Victoria

2024

Chronic states of iron deficiency and excess in combination with erastin: An *in-vitro* study of acute monocytic leukemia (THP-1 cells).

By

Zachariah A. H. Fenniri

Supervisory Committee

Dr. Patrick B. Walter, Supervisor

Department of Biology, University of Victoria

Dr. Jürgen Ehlting, Supervisor

Department of Biology, University of Victoria

2024

Abstract

Iron is essential for numerous biological processes, due to its inherent capacity to transfer electrons. This chemical feature is a double-edged sword, as excess iron catalyzes the formation of reactive oxygen species (ROS) that have potential to cause cellular damage and induce ferroptosis – an iron-dependent form of cell death. Dysregulated iron homeostasis, in favour of accumulation, is a central feature of highly proliferative leukemias, as it enables the required energy metabolism and biosynthesis for unrestrained proliferation. Iron deprivation through the use of iron chelators and the induction of ferroptosis are two potential avenues of clinical antileukemic treatment. The present study aimed to examine the effects of chronic states of iron deficiency and excess in THP-1 cells, an *in-vitro* model of acute monocytic leukemia (AMoL). Moreover, this study sought to examine the effects of these chronic iron states on THP-1 cell resistance to erastin, a compound that induces ferroptosis in many cells, but is largely ineffective in leukemic cell lines. THP-1 cells were cultured in various concentrations of ferric citrate or deferoxamine (DFO), a clinical iron chelator, for 96 hours to simulate chronic states of iron excess and deficiency, respectively. Following 72 hours of treatment, cells were administered erastin for the final 24 hours of treatment. Cell death, metabolic activity, and intracellular glutathione (GSH), a pivotal antioxidant, were quantified. Moderate to high doses of DFO induced marked cell death, as well as a notable reduction in metabolic activity and intracellular GSH. THP-1 cell resistance to erastin was partially attenuated by ferric citrate treatment, evidenced by a small but consistent iron-dose dependent increase in cell death. Similarly, intracellular GSH showed a subtle, insignificant iron-dose dependent reduction in erastin-treated cells. Metabolic activity in the surviving cells was unaffected. DFO is shown to act synergistically with erastin in THP-1 cells, inducing a significant increase in cell death, and in the surviving cells, a reduction in metabolic activity. Likewise, intracellular GSH increases in the surviving cells of this cotreatment. Taken together, the present study demonstrates the robustness of THP-1 cells in states of iron excess and their sensitivity to iron deficiency. It also provides novel evidence of a synergy between DFO and erastin, and of ferric citrate attenuating THP-1 cell resistance to erastin.

Table of Contents

List of Figures

List of Abbreviations

ADP: Adenosine diphosphate

AL: Acute Leukemia

ALL: Acute lymphocytic leukemia

AML: Acute myeloid leukemia

AMoL: Acute monocytic leukemia

ANOVA: Analysis of variance

ATCC: American Type Culture Collection

ATP: Adenosine triphosphate

BCL-2/XL: B-cell lymphoma 2/XL

BRCA1/2: Breast Cancer Susceptibility Gene 1 and 2

BSA: Bovine serum albumin

CD163: Cluster of differentiation 163

CD91: Cluster of differentiation 91

Cl^-: Chloride anion

CL: Chronic leukemia

CLP: Common lymphoid progenitor

CMP: Common myeloid progenitor

CO_2: Carbon dioxide

CoQ: Ubiquinone

dATP: Deoxyadenosine triphosphate

DFO: Deferoxamine

DFP: Deferiprone

DFX: Deferasirox

DMSO: Dimethylsulfoxide

DMT1: Divalent metal transporter 1

DNA: Deoxyribonucleotide triphosphate

DTNB: 5,5’-dithiobis-2-nitrobenzoic acid

EDTA: Ethylenediaminetetraacetic acid

ER: Endoplasmic reticulum

ETC: Electron transport chain

FBS: Fetal bovine serum

Fe-S cluster: Iron-sulfur cluster

Fe^{2+}: Ferrous iron

Fe^{3+}: Ferric iron

$Fe^{3+}{}_2$-$Y^{\bullet}$: Diferric tyrosyl radical

Fe^{4+}: Ferryl iron

FPN: Ferroportin

FSP1: Ferroptosis suppressor protein 1

FT: Ferritin

FTH: Ferritin heavy-chain

FTL: Ferritin light-chain

GPX4: Glutathione peroxidase 4

GR: Glutathione reductase

GSH: Reduced glutathione

GSSG: Oxidized glutathione

H_2O_2: Hydrogen peroxide

HCl: Hydrochloric acid

HIF: Hypoxia-inducible factor

HNO_3: Nitric acid

HO^-: Hydroxide anion

HO-1: Heme oxygenase 1

$HO^{\bullet}$: Hydroxyl radical

HSC: Hematopoietic stem cell

ICT: Iron chelation therapy

IMP: Mobilferrin

IMS: Intermembrane space

IRE: Iron-response element

IRP1/2: Iron-responsive element-binding proteins 1 and 2

K_2HPO_4: Potassium phosphate

LIP: Labile iron pool

LOX: Lipoxygenase

MAPK: Mitogen-activated protein kinase

Mb: Megabases

MEP: Megakaryocyte-erythrocyte progenitor

MPS: Mononuclear phagocyte system

mROS: Mitochondrial reactive oxygen species

Na_2HPO_4: Sodium phosphate

$NAD(P)^+$: Oxidized nicotinamide adenine dinucleotide (phosphate)

NAD(P)H: Reduced nicotinamide adenine dinucleotide (phosphate)

NaOH: Sodium hydroxide

NK Cell: Natural killer cell

NOS: Nitric oxide synthase

NTBI: Non-transferrin bound iron

O_2: Molecular oxygen

$O_2^{\bullet-}$: Superoxide

OMM: Outer mitochondrial membrane

PBS: Phosphate buffered saline

PI3K: Phosphatidylinositol-3-kinase

PIP_3: Phosphatidylinositol-3,4,5-triphosphate

PKB: Protein kinase B

PL: Phospholipid

PMA: Phorbol 12-myristate 13-acetate

PUFA: Polyunsaturated fatty acid

QQ plot: Quantile-quantile plot

RNR: Ribonucleotide reductase

ROS: Reactive oxygen species

RPMI: Roswell Park Memorial Institute

STEAP1/3: Six-transmembrane epithelial antigen of prostate 1 and 3

TF: Transferrin

TFR1/2: Transferrin receptor 1 and 2

THP-1: Tohoku Hospital Pediatrics 1

TME: Tumour microenvironment

UV: Ultraviolet

VDAC: Voltage-dependent anion channels

WHO: World Health Organization

ZIP8/14: Zinc-regulated and iron-regulated transporters 8 and 14

Acknowledgments

First and foremost, I must extend my deepest appreciation to Dr. Patrick Walter. I am so grateful for your willingness to offer me this opportunity and become an ever-important mentor of mine – within and beyond the campus grounds. Those who know you well are conscious of your endless passion for science, and ease with which you navigate day-to-day life. Thank you for your unwavering support.

To Dr. Jürgen Ehlting, I extend my gratitude for your support throughout this project. You are a great scientist and a joy to be around. Thank you for consistently providing a rational, alternate perspective.

To Sarah Lane… goodness me. You are astonishingly compassionate, supportive and a truly effervescent personality to be around, not to mention your wealth of knowledge. Your passion for science and willingness to support your fellow scientists (even the naïve ones like me) are immeasureable. The Ehlting Lab would not be what it is without you and I am absolutely positive that you will go on to make lasting impacts wherever you end up. I'm glad I caught you near the end of your time here!

To everyone in the Walter and Ehlting Labs, thank you for your supportive, accepting energy and for all the time we've spent in lab meetings hashing out our respective projects (often in great stress).

To Dr. Raad Nashmi, thank you for extending your lab space to me for this project. Your support does not go unnoticed.

1.0 Introduction

Cancers are diseases of proliferation, resulting from genetic mutations that induce dysplastic cellular growth and replication (Visvader, 2011). Among them are leukemias, a heterogenous group of blood cell malignancies. Cancer, as a broad disease of many types, remains a leading cause of death globally and leukemias, particularly acute leukemias (AL), are among the most common lethal cancers (*Cancer*, 2022). Iron is an indispensable micronutrient, integral to the function of numerous proteins and enzymes in processes including DNA synthesis and repair, cellular metabolism, and hematopoiesis (Abbaspour et al., 2014). The accumulation of iron, through dysregulated iron homeostasis, is crucial to the proliferative potential of leukemias and all cancers, more broadly (Basak & Kanwar, 2022).

1.1 Iron Necessity and Toxicity

Although abundant on earth, absorbable forms of iron can be a limiting nutrient in many biological systems – iron readily interacts with oxygen to form iron oxides, which are insoluble and biologically incompatible (Abbaspour et al., 2014). The necessity of iron stems from its ability to take part in electron transfers – that is, its capacity to undergo oxidation-reduction (redox) reactions. Iron, a transition metal, can exist in oxidation states of -2 to +6 but is typically limited to ferrous (Fe^{2+}), ferric (Fe^{3+}), and ferryl (Fe^{4+}) states in biological systems (Torti et al., 2018). Much of the functional iron in the human body resides in heme, a metallobiomolecule that contains an intricate coordination complex with Fe^{2+} (Reedy & Gibney, 2004). Heme is a prosthetic group in many proteins essential to electron transfer, reaction catalysis, and most notably, oxygen transport – 85% of heme is found in hemoglobin, the oxygen transport protein essential to respiration (Bartels & Baumann, 1998). Non-heme iron tends to combine with inorganic sulfide, forming aptly named iron-sulfur (Fe-S) clusters. These are, like heme, versatile prosthetic groups that are essential to various proteins whose function relies on the transfer of electrons (Johnson et al., 2005).

One of the essential iron-dependent cellular processes is that of ribonucleotide reductase (RNR) – the ubiquitous cytosolic enzyme that catalyzes the rate-limiting step of DNA synthesis. RNR, through a diferric tyrosyl radical (Fe^{3+}_2-$Y^{\bullet}$) cofactor, reduces ribonucleotides (including adenosine triphosphate [ATP]) to DNA-precursor deoxyribonucleotides (such as deoxyadenosine triphosphate [dATP]) and thereby enables progression from G_1 to S phase in the cell cycle (Puig et al., 2017). Other aspects of basic cellular metabolism are also largely iron-dependent. Cytochromes A, B, C, and D are all redox-active hemoproteins (that is, proteins containing heme) essential to aerobic respiration and overall mitochondrial function (Reedy & Gibney, 2004). Complex IV of the electron transport chain (ETC) in eukaryotic mitochondria, also known as Cytochrome C oxidase, contains two heme groups to help catalyze the transfer of electrons from cytochrome C to molecular oxygen (O_2), forming water (Michel et al., 1998). Complex I of the ETC contains eight Fe-S clusters, and Complex II and III contain both heme groups and Fe-S clusters (Xu et al., 2013). Aconitase, responsible for catalyzing the interconversion of Krebs cycle intermediates citrate and isocitrate, contains an Fe-S cluster at its catalytic centre (Kim et al., 2023).

Protection from oxidative stress in the cell is, in part, provided by heme-containing peroxidases like catalase, which reduces hydrogen peroxide (H_2O_2) to water and O_2 (Alfonso-Prieto et al., 2009). Some oxidoreductases, including nitric oxide synthase (NOS), also employ heme groups as their source of reductive power (Förstermann & Sessa, 2012). Central to processes including the metabolism of foreign compounds and vitamin D_3 synthesis is the vast cytochrome P450 enzyme family, composed of numerous hemoproteins (Nebert & Russell, 2002).

The chemical properties of iron are as harmful as they are required. Iron can participate in reactions that produce reactive oxygen species (ROS), molecules that, as the name suggests, are unstable compounds that can take part in unwanted cellular reactions by reason of their instability. One such avenue is the Fenton reaction (Figure 1), where Fe^{2+} reacts with a peroxide (R-OOH) to produce a highly reactive hydroxyl radical ($HO^{\bullet}$). Fe^{3+} generated by the Fenton reaction can be recycled through the

Haber-Weiss reaction (Figure 1) upon reaction with superoxide ($O_2^{\bullet -}$), a by-product of normal cellular metabolism. This step regenerates Fe^{2+} that can cycle back through the Fenton reaction, producing more toxic $HO^{\bullet}$ (Torti et al., 2018).

$$Fe^{2+} + H_2O_2 \longrightarrow Fe^{3+} + HO^- + HO^{\bullet} \quad \textbf{(Fenton Reaction)}$$

$$Fe^{3+} + O_2^{\bullet -} \longrightarrow Fe^{2+} + O_2$$

(Haber-Weiss Reaction)

$$O_2^{\bullet -} + H_2O_2 \xrightarrow{Fe^{2+}/Fe^{3+}} O_2 + HO^- + HO^{\bullet} \quad \textbf{(Net Haber-Weiss Reaction)}$$

Figure 1. Fenton and Haber-Weiss reactions. In states of iron excess, these reactions are a prominent source of elevated intracellular ROS, which have implications in DNA damage, protein misfolding, inflammation, and cell death.

ROS are very important cell-signaling compounds and must be kept in tight equilibrium to avoid their deleterious effects (Finkel, 2011; Forman et al., 2010). Elevated ROS concentrations are conducive to tumorigenesis, most notably by virtue of increased DNA damage and frequency of mutation, introducing genetic instability (Kirtonia et al., 2020; Moloney & Cotter, 2018). Epidemiological studies support a positive association between various biomarkers of increased body iron levels (e.g. heightened serum transferrin saturation, elevated heme intake, frequency of blood transfusions) and cancer incidence, likely as a result of iron's pro-oxidative nature (Fonseca-Nunes et al., 2014; Hjalgrim et al., 2007; Stevens et al., 1994; T. Wu et al., 2004).

1.2.1 Overview of Cancer

Cancer is among the most maleficent threats to global health today. In Canada, it is the leading cause of death: two in five Canadians are estimated to develop cancer in their lifetime (*Cancer Statistics at a Glance*, n.d.). Cancer comprises over 200 distinct diseases, all of which arise from genetic mutations that are largely spontaneous, as

opposed to inherited (Schär, 2001). ROS are by-products of endogenous metabolism and inflammation that have the potential to inflict oxidative DNA damage (Kirtonia et al., 2020). Environmental stresses like ultraviolet (UV) radiation (sunlight exposure), viral infections, and disruptive compounds in tobacco products are similarly genotoxic (Fontham et al., 2009; Montesano & Hall, 2001). Cells are estimated to endure on the order of 10^4-10^5 spontaneous DNA damaging events every day (Yousefzadeh et al., 2021). The spontaneity of tumorigenic DNA damage introduces mutational heterogeneity between patients and within individual tumours that burdens scientists and clinicians when developing and implementing effective diagnostic tools and treatments for cancer (Salk et al., 2010). Yet, there do exist commonalities between cancer subtypes that simplify the classification and pursuit of these diseases. Genetic perturbations that promote tumorigenesis most often occur in proto-oncogenes, tumour suppressor genes, and DNA repair genes. Proto-oncogenes, genes that encode proteins central to cell proliferation and survival, become tumorigenic *oncogenes* upon garnering gain-of-function mutations (Todd & Munger, 2006). The oncogenic growth-signaling protein Ras, for example, activates diverse signalling cascades that are often constitutively active when mutated (Prior et al., 2020). Tumour suppressor genes encode proteins involved in regulating cell proliferation, including the infamous cell cycle arrest protein p53. Known as the 'guardian of the genome', p53 is mutated in over half of human cancers (Sherr, 2004). DNA repair genes encode proteins that, naturally, respond to DNA damage. These include notable genes like *Breast Cancer Susceptibility Gene 1* and *2* (*BRCA1/2*), which encode key proteins in the DNA damage response (Armstrong et al., 2019).

Excluding common tumorigenic mutations, there exist eight generally accepted characteristics or "hallmarks" of cancer. These include sustained proliferative signalling, resisting cell death, deregulating cellular energetics, enabling replicative immortality, evasion of growth suppressors, activating invasion and metastasis, inducing angiogenesis, and avoiding immune destruction (Hanahan & Weinberg, 2000, 2011). Genome instability and mutation, as well as chronic inflammation, are denoted *cancer-*

enabling characteristics (Hanahan & Weinberg, 2011). While a cancer cell may not possess all the aforementioned characteristics, they outline the transformation of a normal cell into one with malignant properties – once a highly differentiated building block within the host organism, evolved through genetic aberration into a seemingly unrelated entity with one goal: to mercilessly proliferate.

1.2.2 Overview of Acute (Monocytic) Leukemia

Leukemias are cancers of the blood and bone marrow – conditions characterized by the accumulation of genetically aberrant hematopoietic cells with the acquired capacity to rapidly proliferate. Generally, leukemic subtypes are classified based on 1) the rapidity of their proliferation, and 2) the branch of hematopoiesis they stem from. Chronic leukemias (CLs) develop gradually and are, in large part, treatable diseases (Hallek, 2017; Jabbour & Kantarjian, 2018). Acute leukemias (ALs) are much more rapid, aggressive conditions with worse prognoses that involve the dysregulated proliferation of immature (that is, undifferentiated) hematopoietic cells, referred to as 'blasts' (Rose-Inman & Kuehl, 2017). As their titles suggest, acute lymphocytic leukemias (ALLs) involve cells of the lymphoid branch of hematopoiesis, while acute myeloid leukemias (AMLs) involve cells of the myeloid branch (see Figure 2) (Rose-Inman & Kuehl, 2017). ALs, according to the World Health Organization (WHO), are classified by the presence of at least 20% blast cells in the bone marrow or peripheral blood (Swerdlow et al., 2008). For reference, healthy bone marrow normally contains approximately 1-5% blast cells (Masarova et al., 2021).

AML is a heterogenous collection of conditions that makes up nearly a quarter of diagnosed leukemias, globally (Dong et al., 2020). Within these myeloid cell malignancies is a condition known as acute monocytic leukemia (AMoL), a condition in which at least 80% of the blast cell population are of monocytic lineage (Varotto et al., 2022). These cells are precursors to macrophages and dendritic cells, both of which are essential to innate immune function (See Figure 2). Monocytes circulate the blood and spleen and respond to tissue injury or infection through cell surface-expressed pattern

recognition receptors (Ginhoux & Jung, 2014). Monocytes and macrophages are members of the mononuclear phagocyte system (MPS), a crucial branch of innate immunity responsible for engulfing (phagocytizing) pathogens and cellular debris, and recycling nutrients (Hume, 2006). While AMLs occur in all ages, they are the most common ALs in adults and prognosis worsens dramatically with age (Dong et al., 2020). Due to the aggressive nature of these conditions, they require immediate treatment – affected individuals will otherwise die within months or even weeks (Weber et al., 2021). In the United States, AMLs have a mean 5-year survival rate of 32%, while the AMoL subtype has a mean 5-year survival rate of 27% (*SEER Cancer Statistics*, 2023). Patients with AML suffer from dysfunctional hematopoiesis and a subsequent decrease in functional myeloid cells, including erythrocytes, which can temporarily heighten systemic iron levels to a state of primary iron overload (Vinchi et al., 2020). Conversely, experiencing chronic fatigue due to anemia, frequent bleeding and infection are common symptoms of the disease (Weber et al., 2021). To combat insufficient blood cell production, AML patients frequently require red blood cell transfusions, which often result in secondary iron overload and a vicious cycle of excess iron administration that often disproportionally favours malignant cells (Kaphan et al., 2020).

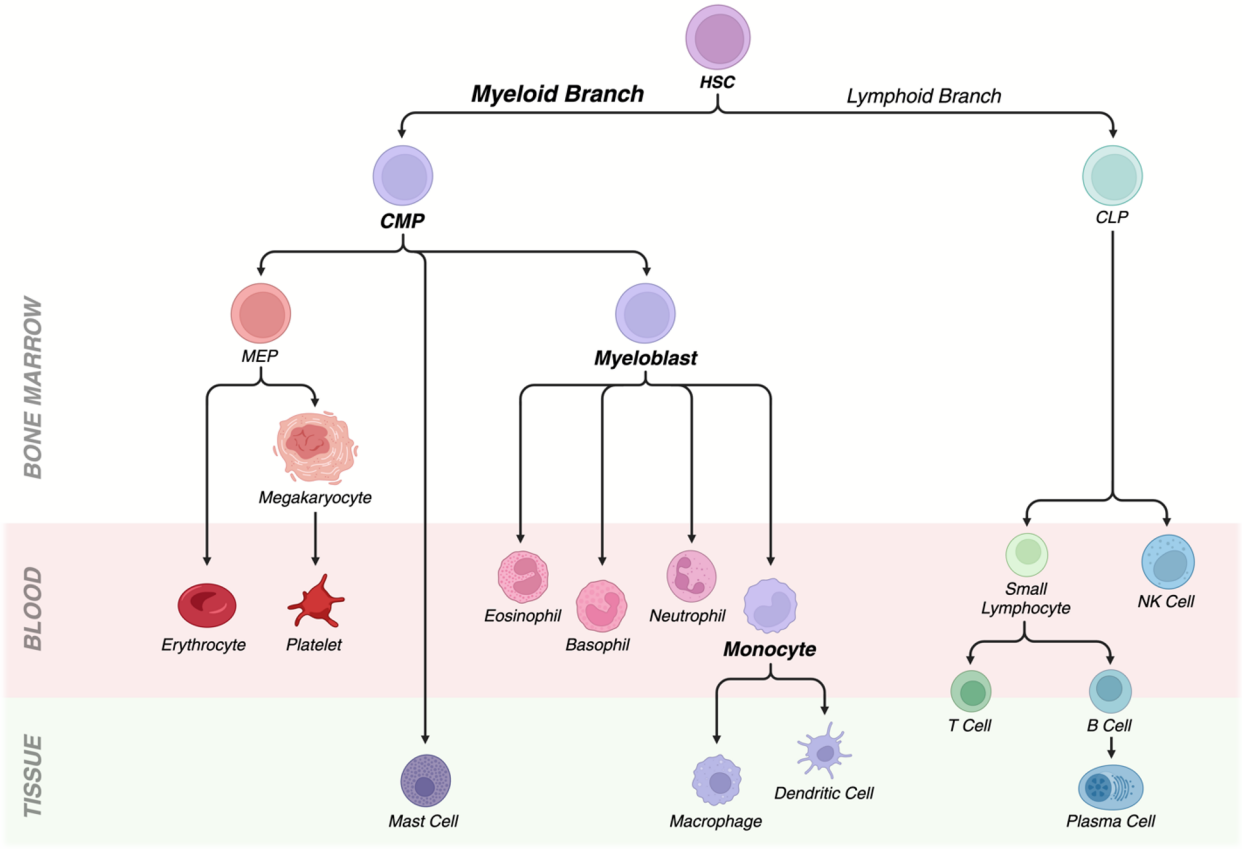

Figure 2. A simplified schematic of hematopoiesis. The fundamental pathways of hematopoietic stem cell (HSC) differentiation and prominent tissues of cell residence are outlined. Leukemias occur as a result of tumorigenic mutations in cells of the hematopoietic lineage and are, in part, classified based on their state of differentiation. CMP, common myeloid progenitor; CLP, common lymphoid progenitor; MEP, megakaryocyte-erythrocyte progenitor; NK Cell, natural killer cell. Created using BioRender.

A common *in-vitro* model of AMoL and AL, more broadly, are Tohoku Hospital Pediatrics 1 (THP-1) cells – transformed monocytic cells obtained from the blood of a one-year old boy with acute monocytic leukemia (Tsuchiya et al., 1980). These cells are hematopoietically immature and readily differentiate to adherent, macrophage-like cells upon stimulation with phorbol 12-myristate 13-acetate (PMA) (Åbrink et al., 1994). According to one complete genomic analysis of THP-1 cells, which identified 119 aberrant regions on autosomal chromosomes, these cells have homozygous deletions amassing to 4.6 million bases (4.6 Mb) (Adati et al., 2009). THP-1 cells have a 26-base

deletion in of the *TP53* gene, responsible for encoding p53 (Sugimoto et al., 1992). As was previously mentioned, over 50% of cancers are p53-mutants. In normal cells, p53 is activated in response to DNA damage and initiates the transcriptional programs of cell cycle arrest, senescence (dormancy), DNA repair and apoptosis (Marei et al., 2021). The aforementioned genomic analysis discovered a short (kilobases) deletion in the *TP73* gene, responsible for encoding p73 (Adati et al., 2009). p73 is homologous to p53 and has overlapping roles, in part due to their structural similarity and its ability to bind p53 promotor regions on DNA (Levrero et al., 2000). THP-1 cells also have homozygous deletions of the *CDKN2A* and *CDKN2B* genes, which encode the cell cycle arrest proteins p16 and p15, respectively (Adati et al., 2009; Foulkes et al., 1997; Xia et al., 2021). Further, THP-1 cells are homozygous mutants of the *PTEN* gene, another crucial tumour suppressor (Adati et al., 2009). PTEN is a lipid phosphatase that hydrolyzes the 3-position phosphate of phosphatidylinositol-3,4,5-triphosphate (PIP_3), in opposition to oncogenic signalling protein phosphatidylinositol-3-kinase (PI3K), thereby inhibiting the activation of protein kinase B (PKB) (Hopkins et al., 2014). When (constitutively) active, the PI3K-PKB axis has potent antiapoptotic, proliferative function. In combination, THP-1 cells have eliminated pivotal antiproliferative, apoptotic machinery that allows for unrestrained growth and proliferation.

1.3 Iron Homeostasis

To understand how leukemic cells dysregulate cellular iron hemostasis to their advantage, the processes of normal iron homeostasis are outlined in this section. While humans typically ingest 10-20 mg of dietary iron every day, only 1-2 mg is absorbed. Likewise, 1-2 mg is lost every day via epithelial desquamation, sweat or bleeding (Abbaspour et al., 2014). On the apical surface of enterocytes in the small intestine, dietary iron is absorbed via divalent metal transporter 1 (DMT1), a widely expressed cellular membrane transporter of Fe^{2+}, predominantly, as well as manganese (Mn^{2+}) (Ganz, 2013). The mechanism of dietary heme-iron absorption remains enigmatic, although it is established that heme oxygenase 1 (HO-1) degrades absorbed heme, liberating Fe^{2+} (Dutt et al., 2022). At the basal membrane of the enterocyte, Fe^{2+} is re-

oxidized to Fe^{3+} and exported out of the cell through ferroportin (FPN), the ubiquitous iron efflux transporter (Ganz, 2013). Once exported, two Fe^{3+} ions are loaded onto transferrin (TF), the vertebrate iron-carrier protein, for systemic circulation and delivery (Kawabata, 2019).

TF-bound iron is absorbed upon binding transferrin receptor 1 (TFR1) or the lesser expressed transferrin receptor 2 (TFR2) on the cell surface. Binding triggers endocytosis of the TF-TFR complex and release of the two Fe^{3+} ions, followed by their reduction to Fe^{2+} by metalloreductases like six-transmembrane epithelial antigen of prostate 3 (STEAP3). Fe^{2+} is transported out of the endosome by DMT1, thereby entering the metabolically active labile iron pool (LIP) in the cytosol (Ganz, 2013; Kawabata, 2019). Aside from DMT1, there are various mechanisms through which cells influx non-transferrin-bound-iron (NTBI). Fe^{2+} is transported into various cell types by zinc-regulated and iron-regulated transporters 8 (ZIP8) and 14 (ZIP14), which synonymously transport zinc (Zn^{2+}) and cadmium (Cd^{2+}) (Guerinot, 2000). A rather unique mechanism is the ($beta_3$) integrin-mobilferrin (IMP) pathway – a route of Fe^{3+} transport across the plasma membrane of certain cell types, including enterocytes and even leukemic cells (Conrad et al., 1994, 2000).

In the cell, excess iron is stored in ferritin (FT), the ubiquitous iron-storage protein, which can inertly store upwards of 5000 Fe^{3+} atoms in a nanocage structure (Brown et al., 2020; Jian et al., 2016). Fe^{3+} can then be accessed through a ferritin-specific autophagy, aptly named ferritinophagy (Plays et al., 2021). Intracellular iron homeostasis is controlled by iron-responsive element-binding proteins 1 (IRP1) and 2 (IRP2), which bind iron-response elements (IREs) on untranslated regions of mRNA to regulate the translation of iron import proteins (e.g. TFR1, DMT1), storage proteins (FT), and export proteins (FPN). In response to a reduction in available iron, IRP1 and 2 undergo conformational changes that promote binding to IREs, heightening TFR1 translation and decreasing FT and FPN production. Similarly, excess intracellular iron structurally alters IRP1 and 2, preventing them from binding and exerting an effect on IREs (Cardona & Montgomery, 2023). Free oxygen and ROS, too, are regulators of IRP

binding capacity. As is summarized in Figure 3, iron homeostasis is created by a constellation of tightly regulated mechanisms. Many of these processes are hijacked by genetically aberrant leukemic cells for their proliferative advantage.

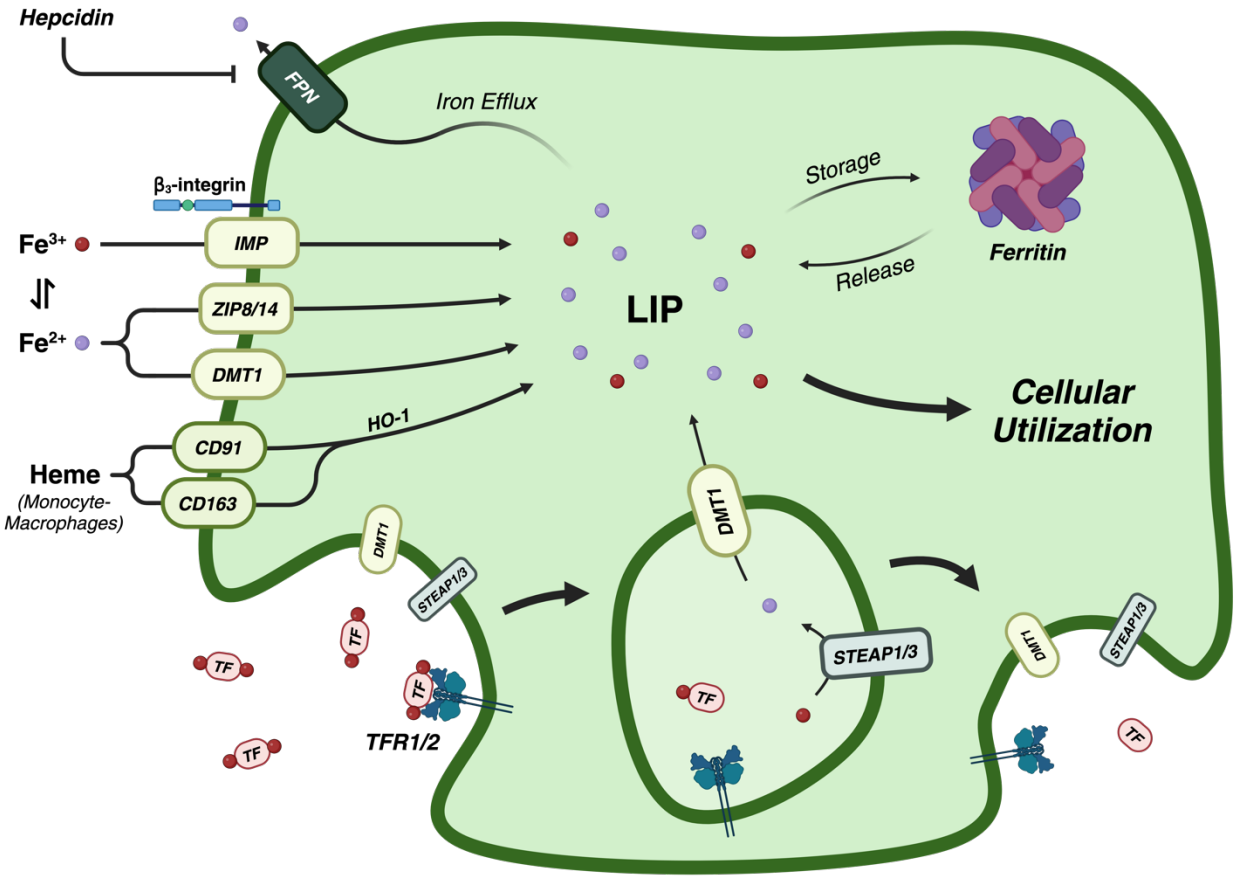

Figure 3. Summary of cellular iron homeostasis, with a focus on relevant influx and efflux mechanisms. Regulation of protein translation by iron-responsive element-binding proteins 1 and 2 (IRP1/2) is not shown. LIP, labile iron pool; FPN, ferroportin; IMP, mobilferrin; ZIP8/14, zinc-regulated and iron-regulated transporters 8 and 14; DMT1, divalent metal transporter 1; CD91, cluster of differentiation 91; CD163, cluster of differentiation 163; HO-1, heme-oxygenase 1; STEAP1/3, six-transmembrane epithelial antigen of prostate 1 and 3; TF, transferrin; TFR1/2, transferrin receptor 1 and 2. Created using BioRender.

1.4 Iron Dysregulation and Leukemia

Dysregulated iron homeostasis is associated with the incidence of leukemia (Hagag et al., 2018; Kennedy et al., 2014) and like all cancers, this is largely believed to

result from Fenton chemistry, the subsequent production of ROS, and their damaging effects on DNA (Torti et al., 2018; C. Zhang & Zhang, 2015). Notably, hematopoiesis relies on the presence of iron and the subsequent production of ROS, which act as signal messengers in the regulation of HSCs and the bone marrow microenvironment (Ludin et al., 2014). However, dysregulated iron redox balance promotes the transformation of HSCs and other hematopoietic cells by increasing the frequency of DNA damage and erroneous repair (Hole et al., 2013; Rassool et al., 2007). Generally speaking, normal cells upregulate the influx of iron in hypoxic conditions via hypoxia-inducible transcription factors (HIFs) (Semenza, 2001) and in response to injury (Wessling-Resnick, 2010). All cancer cells, though, have a greater demand for iron to heighten biosynthesis and support proliferation. Due to their origins in hematopoiesis, as well as their high concentration in the blood, leukemic cells particularly favour the accumulation of iron by increasing iron influx and storage, while decreasing iron efflux (Wang et al., 2019).

TFR1 is overexpressed in all leukemic cells, with a greater prevalence in AMLs than in ALLs (Liu et al., 2014; Pande et al., 2016). Similarly, the expression of TFR2 is heightened in AMLs (Kawabata et al., 2001). Influx of NTBI via DMT1, STEAP-family reductases, ZIP8 and ZIP14, and beta$_3$-integrin-associated IMP are all subject to potential dysregulation in leukemic cells (Alluri et al., 2021; M. E. Conrad et al., 1994; Guo et al., 2021; Moreaux et al., 2012). Clusters of differentiation 163 (CD163) and 91 (CD91) are scavenger receptors involved in the uptake of heme-bound iron, expressed on monocytes and macrophages (Brown et al., 2020; Lizier et al., 2016). CD163 is considered a specific marker of AMoL (Garcia et al., 2008). In favour of iron accumulation, both subunits of FT, ferritin light-chain (FTL) and heavy-chain (FTH) are often subject to overexpression in AML (Bertoli et al., 2019; Zolea et al., 2015). Likewise, FPN is often downregulated in leukemic cells, potentially as a result of autocrine hepcidin signaling (Wang et al., 2019). In concert, the aforementioned homeostatic changes promote a systematic overaccumulation of iron, and act as a driving force in the proliferative success of leukemic cells.

1.5 Iron Excess and Ferroptosis

Upon exposure to excessively elevated iron levels, a cell faces considerable oxidative stress that, without sufficient antioxidant protection, may ultimately result in cell death. This avenue, known as ferroptosis, is a recently discovered iron-dependent mode of cell death that is morphologically, biochemically, and genetically different from all other forms of cell death and recycling – including apoptosis, necrosis, necroptosis, and autophagy (Dixon & Stockwell, 2019; Li et al., 2020; Xie et al., 2016; W. S. Yang & Stockwell, 2016). Ferroptosis occurs through the peroxidation of membrane lipids and a subsequent accumulation of lipid ROS, resulting in membrane stiffening and nanopore formation, loss of ionic homeostasis, and eventual membrane failure (Hirata et al., 2023). The accumulation of iron and the iron-catalyzed formation of ROS, primarily via Fenton chemistry, are prerequisites of this process (Dixon & Stockwell, 2019). The initial discovery of the ferroptotic mechanism arose from experiments with erastin, a compound previously known to induce non-apoptotic cell death in Ras-mutant cancer cells (Dixon et al., 2012). The primary action of erastin is the inhibition of system x_C^-, a cystine/glutamate antiporter that imports cystine (dimeric oxidized cysteine) into the cell in exchange for glutamate (Bridges et al., 2012). System x_C^- is at the forefront of acquiring cysteine, which, in the form of cystine, is fairly abundant (approximately 50 μM) in circulation (Combs & Denicola, 2019). Cysteine is a limiting substrate in the synthesis of glutathione (GSH), a primary mediator of cellular redox balance (Sun et al., 2018). GSH is the required co-factor of glutathione peroxidase 4 (GPX4), a selenoprotein (selenium-containing protein) that reduces (toxic) lipid peroxides to (harmless) lipid alcohols, subsequently oxidizing GSH to glutathione disulfide (GSSG) (Conrad & Friedmann Angeli, 2015). Thus, erastin induces ferroptosis by depleting cells of cysteine, hampering the synthesis of GSH and inhibiting the function of GPX4, which consequently leads to an artificial increase in membrane lipid ROS and the induction of ferroptosis (Figure 4) (Zhao et al., 2020).

Dixon & Stockwell (2019) describe three fundamental characteristics of ferroptosis: first, the peroxidation of polyunsaturated fatty acid (PUFA)-containing phospholipids (PLs) that are incorporated in a cellular or subcellular membrane. This

can occur through reactions with iron and soluble ROS, or the action of lipoxygenases (LOXs), which catalyze the formation of lipid peroxides for processes including membrane signalling and lipid mediation (Mashima & Okuyama, 2015; Shah et al., 2018). While lipid peroxidation can occur in any of the cell's lipid membranes, the membrane of the endoplasmic reticulum (ER), the plasma membrane, and the mitochondrial membrane are central to the ferroptotic mechanism (von Krusenstiern et al., 2023). Furthermore, the deletion of genes responsible for activation or incorporation of activated PUFAs into membrane PLs prevents ferroptosis (Doll et al., 2016; Kagan et al., 2016). In other words, there must be a sufficient PUFA-PL density in the membrane for ferroptosis to occur. Second, the presence of redox-active iron (free or as enzymatic co-factor) is required for ferroptotic cell death. Iron chelating compounds like deferoxamine (DFO) can rescue cells from ferroptotic death by interfering with iron-catalyzed lipid peroxidation (Stockwell et al., 2017). Similarly, the downregulation of TFR-mediated iron import can prevent ferroptosis (Gao et al., 2015), as does the inhibition of ferritinophagy, presumably by reducing the amount of available free iron (Hou et al., 2016). The third characteristic is an insufficient prevention and repair of lipid peroxides. The present understanding of intrinsic defense against the accumulation of lipid peroxides and ROS comprises a handful of antioxidant pathways and in many cells, the most critical of these is the aforementioned GSH-GPX4 axis (Kinowaki et al., 2018; Seiler et al., 2008). Functioning independently in parallel to GPX4, ferroptosis suppressor protein 1 (FSP1) is a novel oxidoreductase that, like GPX4, prevents the peroxidation of plasma membrane lipids (Figure 4) (Bersuker et al., 2019). FSP1 reduces oxidized ubiquinone (coenzyme Q_{10}; CoQ) and Vitamin K, both of which (in their reduced forms) trap lipid peroxyl radicals (R-OO$^{\bullet}$), which are precursors to lipid peroxides (Bersuker et al., 2019). FSP1 requires reducing power from reduced nicotinamide adenine dinucleotide (phosphate) (NAD(P)H) and is anchored to the plasma membrane through myristoylation (Doll et al., 2019). This link to the plasma membrane appears to be crucial to the effectiveness of FSP1 in suppressing ferroptosis.

Excluding the aforementioned lipid repair mechanisms, the regulation of ferroptosis is intricately linked to previously described mechanisms of iron influx, efflux, and storage (Dixon & Olzmann, 2024). While the removal of redox-active iron from the cell and its immediate environment can be protective against ferroptosis, iron deprivation can be equally, if not more devastating in leukemic cells. As will be described, depriving leukemic cells of iron through the use of iron-chelating compounds is a compelling, alternative avenue of research and antileukemic treatment.

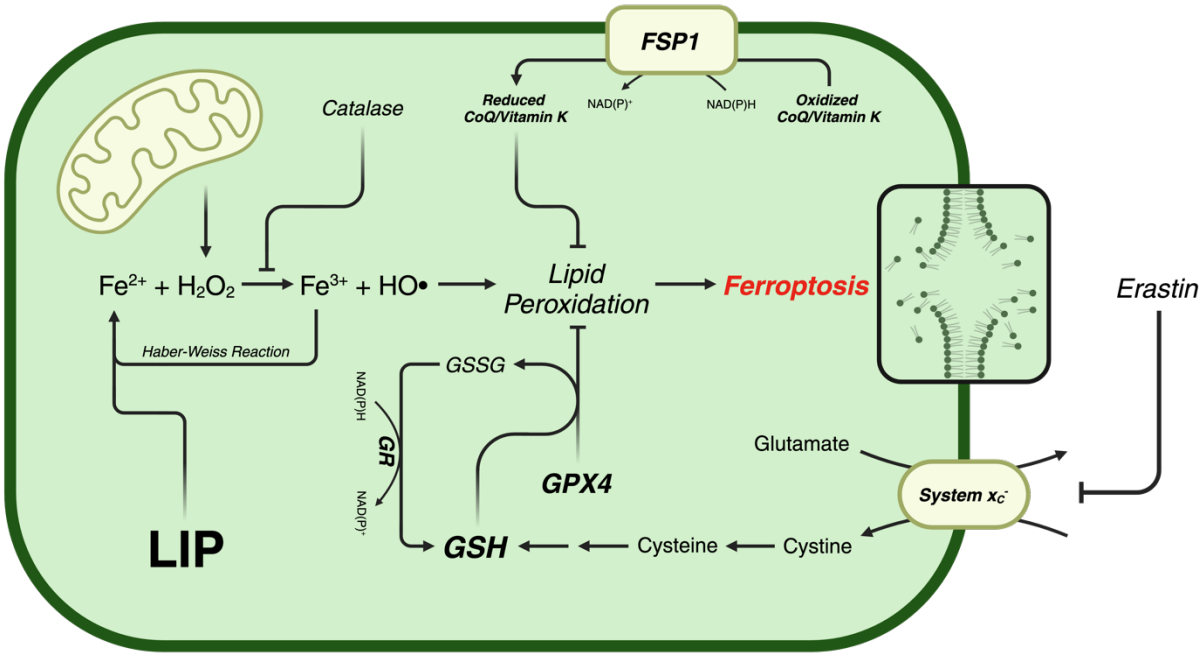

Figure 4. Summary of ferroptosis. Central to the induction of ferroptosis is Fenton reaction-generated ROS, which contributes to the peroxidation of membrane lipids. Catalase catalyzes the conversion of H_2O_2 to H_2O, reducing the iron-catalyzed formation of $HO^{\bullet}$. Ferroptosis suppressor protein 1 (FSP1) and glutathione peroxidase 4 (GPX4) are the frontline lipid peroxide repair mechanisms. Erastin exhausts cellular glutathione (GSH) synthesis by inhibiting the uptake of cystine via system x_C^-. Oxidized glutathione (GSSG) is reduced back to GSH by glutathione reductase (GR). LIP, labile iron pool; NAD(P)H, reduced nicotinamide adenine dinucleotide (phosphate); $NAD(P)^+$, oxidized nicotinamide adenine dinucleotide (phosphate); CoQ, ubiquinone. Created using BioRender.

1.6 Iron Chelation Therapy

The heightened requirement for iron in leukemic cells renders them more sensitive to iron deprivation than their non-transformed counterparts (Wang et al., 2019). This makes for a potential therapeutic avenue: depriving these cells of iron through the use of iron chelators – compounds (natural or synthetic) that bind iron atoms with strong affinity, rendering them inert (Hatcher et al., 2009). Unlike other iron sources, chelator-iron complexes can be excreted (Wang et al., 2019). This feature makes iron chelation therapy (ICT) a bimodal treatment, being antileukemic and reducing the burden of iron overload that often accompanies leukemic disease (Weber et al., 2021). Most chelators contain oxygen, nitrogen, or sulfur atoms that donate electrons to form coordination bonds with a central iron atom (Hatcher et al., 2009). Hexadentate iron chelators have six donor atoms – that is, six atoms with a lone electron pair – that interact in a 1:1 ratio with all six coordination sites of an iron atom (Ma et al., 2012). Conversely, tridentate and bidentate chelators interact with three and two coordination sites, respectively (Ibrahim & O'Sullivan, 2020). At low concentrations, tri- and bidentate chelators may leave coordination sites unbound, allowing for some iron reactivity even in a partially coordinated state (Bogdan et al., 2016).

DFO, a hexadentate chelator produced by certain bacteria (*Streptomyces pilosus*) was the first clinical iron chelator used for the treatment of iron overload and the first to be trialed as a cancer therapy (Estrov et al., 1987; Propper et al., 1977). It has a very short half-life in circulation (5-10 minutes) and is hydrophilic, rendering it largely incapable of crossing the plasma membrane (Ibrahim & O'Sullivan, 2020). Being a hexadentate with high affinity, DFO readily coordinates with all six binding regions of the iron atom (Figure 5). DFO is highly antiproliferative in leukemic cells by indirectly blocking the synthesis of deoxyribonucleotides through the loss of normal RNR function (Furukawa et al., 1992). Subsequent cell cycle arrest at G_1/S phase occurs through a downregulation of $p21^{CIP1/WAF1}$, a protein with antiapoptotic function that positively regulates progression to S phase of the cell cycle (Fu & Richardson, 2007). Moreover, the heme prosthetic group of catalase can no longer be synthesized when iron is deficient, thereby reducing a first-line of cellular antioxidant defense (Yoo et al., 2009).

Aside from inhibiting iron-dependent proteins, iron deprivation is shown to activate diverse cellular apoptotic cell death programs (Koc et al., 2005; Liu & Zhu, 2022; Xue et al., 2021; Yang et al., 2021; Yang et al., 2018). Aside from DFO, deferiprone (DFP), a tridentate chelator, and deferasirox (DFX), a bidentate chelator, are common alternative clinical iron chelators (Saliba et al., 2015). Unlike DFO, these compounds are lipophilic and readily diffuse across the plasma membrane. They, too, have potent antileukemic activity, potentially through similar action to DFO (Shapira et al., 2019; Tataranni et al., 2015).

By sequestering the available iron, iron chelators are removing a fundamental substrate of oxidative stress. This does not simply reduce the formation of ROS, however. Even low doses of DFO, DFP, and DFX significantly increase ROS generation in leukemic cells (Liu & Zhu, 2022; Shapira et al., 2019; Tataranni et al., 2015). Mitochondrial function, particularly in the realm of oxidative phosphorylation via the ETC, relies on iron chemistry – complexes I, II, III, and IV of the ETC rely on Fe-S clusters and heme groups (Xu et al., 2013). Iron deprivation creates an inability to properly transfer electrons and pump protons across the inner mitochondrial membrane, which causes only a partial reduction of oxygen and subsequent formation of mitochondrial ROS (mROS), like $O_2^{\bullet -}$ and H_2O_2, instead of a complete reduction to H_2O (Lenaz, 2012). Interestingly, DFO is shown to cause differentiation of THP-1 cells to functional macrophages, accompanied by a reduction in intracellular GSH (Seo et al., 2006). When supplemented with a *N*-acetyl-cysteine, a precursor to GSH, THP-1 cells no longer underwent DFO-induced differentiation, supporting the notion that ROS modulate cellular differentiation.

Iron chelators, then, exert diverse effects beyond simply reducing cellular iron. ICT is far from perfect, having various adverse side effects and a lack of specificity. These compounds and treatments require further investigation and amelioration for addressing leukemias and cancers, more broadly.

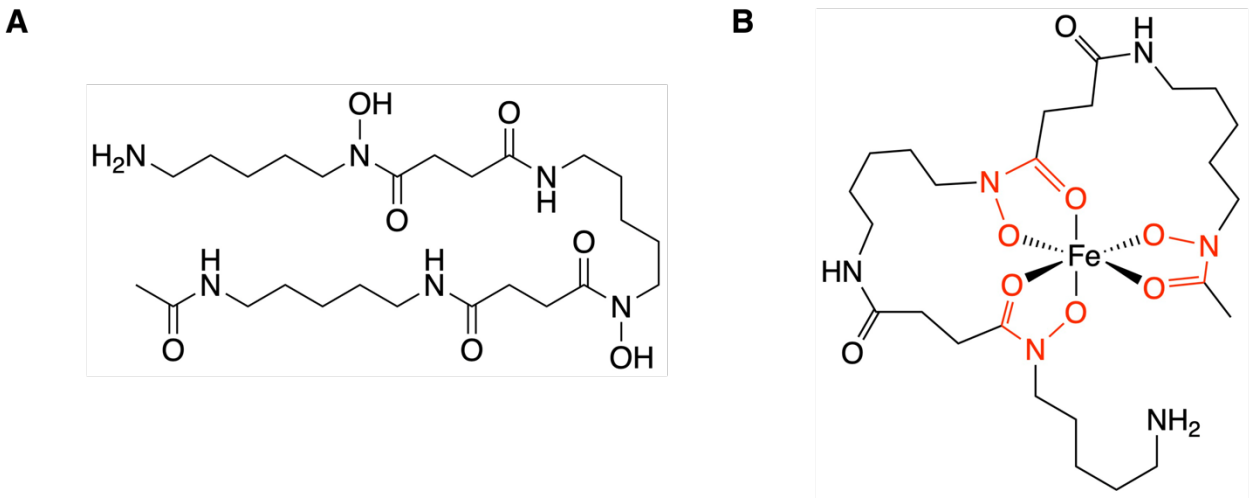

Figure 5. (A) Deferoxamine (DFO). **(B)** DFO-iron hexadentate coordination complex.

1.7 Summary of Objectives

Iron is an essential micronutrient to many biological processes and subsequently, iron deficiency is damaging to normal cellular functioning. Contrary to its necessity, however, iron possesses an inherent toxicity in excess. The pathological relationship of iron chemistry and leukemia is well-documented, but much of its intricacy remains speculative. While therapies for patients with AMoL and other subtypes of AML have improved, as have their survival rates, the burden and lethality of these diseases remain a serious concern in many lives today. A more advanced understanding of the relationship between iron and different AMLs, particularly in regard to therapeutic targets, is important.

To support unrestrained proliferation, leukemic cells favour the accumulation of iron. Depriving leukemic cells of iron using iron chelators like DFO, DFP, or DFX is a promising therapeutic tool that requires further optimization. Indeed, targeting a synergy between a clinical iron chelator that induces an increase in ROS and other anti-leukemic agents may prove to be the most effective method of anti-leukemic iron chelation therapy. Probing for a synergistic relationship between an iron chelator like DFO and a so-called ‘ferroptosis inducer’ like erastin appears contradictory but considering the

potential lethality of DFO in leukemic cells and the GSH-depriving effects of erastin, it is worth investigating as a novel combination therapy.

Targeting the induction of ferroptosis in these iron-accumulated cells is a logical therapeutic avenue in many cancers – it appears, however, that leukemic cells are highly resistant to states of iron excess (Gharagozloo et al., 2008; Kraml et al., 2005; Zheng et al., 2017). Conversely, *in-vitro* studies of iron excess and leukemic cells are typically limited by very acute treatment periods, often less than 24 hours. Examining the effects of chronically elevated iron levels past 24 hours in leukemic cells would provide a more accurate depiction of the tumour microenvironment (TME). An effective antioxidant system is vital to survival in these iron-rich conditions, too, mitigating an otherwise inevitable ferroptotic cell death. The GSH-GPX4 axis is a logical avenue of investigation in iron-resistant leukemic cells. Interestingly, THP-1 cells are among numerous leukemic cells lines with marked resistance to erastin (Kumada et al., 2024; Ye et al., 2019; Yu et al., 2015). The aforementioned *in-vitro* studies did not administer erastin in elevated iron environments, however. Treating cells with erastin in the presence of excess iron may confer a greater effectiveness of erastin and be of better biological significance than simply treating cells with erastin in normal culture media.

The present study seeks to further examine the relationship of iron and THP-1 cells. The objective is to model the effects of iron, from states of iron deprivation to states of iron excess, and potential synergies with erastin. Specifically, this study examines the effects of ferric citrate, a soluble source of Fe^{3+}, and DFO on THP-1 cell death, metabolic activity, and antioxidant response through intracellular GSH levels. Cell death is quantified using trypan blue, a dye that permeates into cells with compromised membrane integrity, a hallmark of cell death (Strober, 2015). Metabolic activity is quantified using an established method based upon resazurin, a compound that reacts with reduced nicotinamide adenine dinucleotide (NADH) and reduced nicotinamide adenine dinucleotide phosphate (NADPH), both of which are essential reducing agents and intermediates of cellular metabolism (Präbst et al., 2017; Singh et al., 2008). A schematic of the resazurin assay is provided (Appendix A). Intracellular

GSH levels are quantified using an established method based on 5,5'-dithiobis-2-nitrobenzoic acid (DTNB) (Rahman et al., 2007). A schematic of the DTNB assay is provided (Appendix B). It is hypothesized that in chronic conditions of iron excess, THP-1 cell viability and metabolic activity will be unaffected. It is further hypothesized that intracellular GSH levels will decrease as doses of iron increase, indicating an iron dose-dependent antioxidant response. DFO is expected to decrease viability, metabolic activity, and GSH content in THP-1 cells. While it is expected that THP-1 cells will be unaffected by erastin treatment alone, it is hypothesized that iron and DFO treatments will increase the effectiveness of erastin as an antileukemic treatment.

2.0 Methods

2.1 Cell Line and Chemicals

THP-1 cells were obtained from the American Type Culture Collection (ATCC). Fetal bovine serum (FBS), glucose, phosphate buffered saline (PBS), AAS iron standard, DFO, resazurin, DTNB, and reduced glutathione (GSH) were all sourced from Sigma-Aldrich. Roswell Park Memorial Institute medium (RPMI 1640, no glutamine), Glutamax, penicillin-streptomycin, sodium pyruvate, beta-mercaptoethanol, dimethylsulfoxide (DMSO), and trypan blue were all sourced from ThermoFisher Scientific. MOPS buffer and ethylenediaminetetraacetic acid (EDTA) were sourced from BioBasic. Sodium hydroxide (NaOH) and hydrochloric acid (HCl) were sourced from Fisher Scientific. Potassium phosphate (K_2HPO_4) and sodium phosphate (Na_2HPO_4) were sourced from EMD. Erastin was sourced from Stem Cell Technologies and MedChemExpress. Citric acid monohydrate was sourced from ACP. Nitric acid (HNO_3) was sourced from Anachemia. Triton X-100 was sourced from PhytoTech Labs. All reagents were ACS grade or equivalent, unless otherwise specified.

2.2 Cell Culturing and Passaging

THP-1 cells were lifted from liquid nitrogen cryopreservation at -80°C, rapidly thawed in a 37°C-water bath and transferred to a 15 mL conical centrifuge tube. To

remove cryopreservation agent (10% DMSO), cells were washed in pre-warmed 37°C RPMI 1640 media, containing 10% FBS, Glutamax (2 mM), glucose (4.5 g/L), sodium pyruvate (1 mM), 1% penicillin-streptomycin (100 U/mL), and beta-mercaptoethanol (50 μM). Cells were cultured in complete RPMI media, in vented 25 cm^2 culture flasks (T-25, Corning). When the cells were determined to have fully recovered from cryopreservation, complete RPMI media without beta-mercaptoethanol was used. Flasks were kept in a humidified incubator maintained at 37°C and 5% CO_2. Cells were passaged every 48-72 hours. During a passage, cells were transferred to a conical tube, from which a representative sample was taken for a cell count performed with trypan blue (0.4% in PBS) and a hemocytometer. After determining the approximate cell density of the flask, the cells were diluted with fresh complete RPMI media to a density of 250,000 cells/mL and the excess cells and media were discarded. The passaged cells were transferred back to a T-25 culture flask and returned to the incubator.

2.3 Experimental Treatments

At an initial density of 250,000 cells/mL, THP-1 cells were treated with varying concentrations of ferric citrate (100 mM citrate, 5 mM AAS iron standard in 2% HNO_3, and 20 mM MOPS; pH 7.4) or DFO (5 mM in PBS). Ferric citrate stock solution was prepared by adding 2.79 mL AAS iron standard to 1.0 mL citrate, dropwise. The solution was a yellow-green colour at this stage. This was followed by the dropwise addition of 1.0 mL MOPS buffer, after which 3.70 mL 1.0M NaOH was added, dropwise, until the solution's colour changed to a golden yellow. If the colour change occurred prior to the complete addition of 3.70 mL NaOH, the remaining NaOH was diluted in 1.5 mL Milli-Q water and added, dropwise. If the colour change had not yet occurred, NaOH was added, dropwise, until the colour change occurred. The remaining volume (1.5 mL - volume of additional NaOH) of Milli-Q water was then added, dropwise. Iron control cells were treated with a citrate-only (blank) solution (100 mM citrate, 20 mM MOPS, 2% HNO_3), prepared using the same protocol described above. The AAS iron standard in 2% HNO_3 was replaced with 2% HNO_3, and the colour changes do not occur as a result. Crucially, preparation of the ferric citrate stock solution and the citrate blank

solution is done with constant, vigorous stirring and pH was monitored and adjusted to a range of 7.2-7.5. DFO control cells are treated with PBS.

Cells were treated with ferric citrate at concentrations of 10 μM, 20 μM, 40 μM, 100 μM, 150 μM, or 200 μM, while DFO treatments were at concentrations of 10 μM, 20 μM, 40 μM, or 100 μM. Following 48 hours (± 2 hours) of treatment, media was refreshed, and treatments were re-applied. Iron and DFO treatments both spanned 96 hours (± 2 hours). Upon determining the treatment conditions of greatest interest for erastin cotreatments, THP-1 cells were treated with ferric citrate (20 μM, 100 μM, or 200 μM) or DFO (20 μM) for 96 hours (± 2 hours), with appropriate controls. After 48 hours (± 2 hours), the media was refreshed, treatments were re-applied, and each treatment condition was split into two wells. Following 72 hours (± 2 hours) of treatment, half of the samples received erastin (20 mM in DMSO) at a final concentration of 40 μM. That is, each treatment condition had an erastin-treated counterpart. During experiments, a separate culture of THP-1 cells was maintained and routinely passaged.

2.4 Trypan Blue Exclusion Assay

Cell death was monitored during routine passages and during experimental treatments. From each cell treatment condition, a 20 μL representative sample was transferred to a microfuge tube with 20 μL of trypan blue solution (0.4% in PBS) and pipetted up and down to mix. From the microfuge tube, 10 μL of the 1:1 mixture was loaded on a hemocytometer. Using phase-contrast microscopy, the number of live (clear) and dead (blue) cells (i.e. the live:dead ratio) were counted in four 1 mm^2 counting grids. The average live cell count of the four grids was multiplied by the dilution factor and grid volume to obtain a total sample cell density in cells/mL.

2.5 Resazurin Metabolic Assay

A resazurin metabolic assay was performed as an indirect measure of THP-1 cell metabolic activity. Samples were centrifuged at 270 x g for five minutes and resuspended in fresh media. In triplicate, 80 μL of each sample was transferred to an

opaque 96-well microplate, followed by the addition of 20 μL of resazurin solution (resazurin powder in PBS, 0.15 mg/mL). Plates were covered with aluminum foil to prevent any light reactions and incubated at 37°C for three hours. Fluorescence of the reaction product (resorufin) was measured at 560 nm in a Perkin Elmer Victor X5 2030 microplate reader. Background fluorescence was subtracted from each value, which was then normalized to cell number. Each technical replicate of the samples treated with ferric citrate contained approximately 125,000 cells, as was determined to be optimal in a preliminary dose-response experiment (Appendix C). As a result of DFO lethality at higher doses and in combination with erastin (40 μM, 100 μM, 20 μM + 40 μM erastin), each technical replicate of DFO-treated samples contained approximately 3,600 cells.

2.6 Intracellular GSH Assay

DTNB was utilized to assess intracellular GSH concentration in THP-1 cells. After washing in PBS, samples were centrifuged at 450 x g and resuspended in ice-cold lysis buffer (50 mM K_2HPO_4, 1.0 mM EDTA, 0.1% v/v Triton X-100; pH 6.5), in which they incubated for 15 minutes on ice. Following cell lysis, samples were centrifuged at 10,000G, at 4°C, for 15 minutes to clear the crude lysate. At this stage, the supernatant (cleared cell lysate) contains small cytosolic peptides, including GSH. The cleared cell lysate was either used immediately or stored at -80°C until used. GSH standards were prepared by dissolving L-GSH in acidic reaction buffer (100 mM Na_2HPO_4, 1.0 mM EDTA; pH 6.5) to 1250 μM and serially diluting to 39.1 μM. In duplicate, 50 μL of GSH standards and cleared cell lysates were transferred to a clear 96-well microplate, followed by 40 μL of basic reaction buffer (100 mM Na_2HPO_4, 1.0 mM EDTA; pH 8.0) and 10 μL of DTNB (4 mg/mL in basic reaction buffer) in each well. Plates were incubated for 15 minutes at 37°C, and absorbance was measured at 405 nm using a Perkin Elmer Victor X5 2030 microplate reader. The GSH concentration of each sample was calculated using a GSH standard curve (Figure 6) and was normalized to protein content using the Pierce BCA Protein Assay.

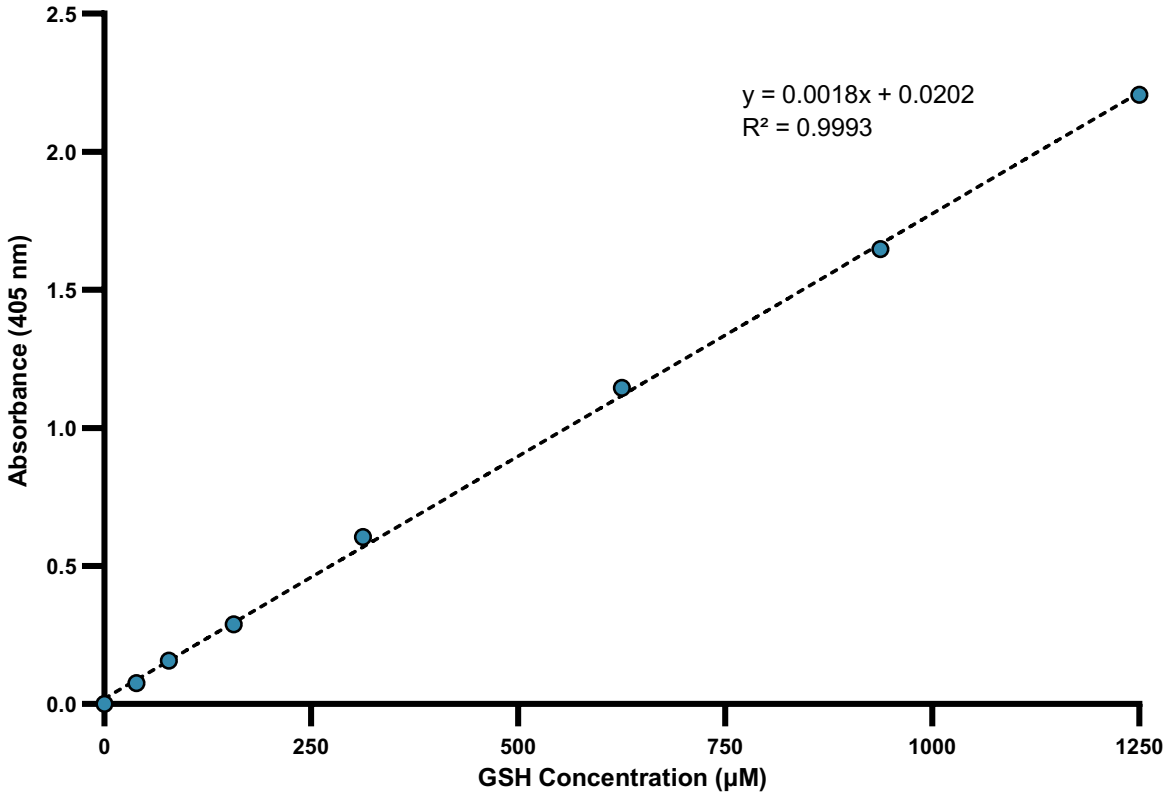

Figure 6. Standard curve of reduced glutathione (GSH) concentrations, used to quantify intracellular GSH from DTNB assay absorbance values. Absorbance was measured at 405 nm in a Perkin Elmer Victor X5 2030 microplate reader. Background absorbance was subtracted.

2.7 Protein Content Determination

A Pierce BCA Protein Assay Kit was used to determine the protein content of cell samples. A standard curve was prepared with 2 mg/mL bovine serum albumin (BSA) diluted in PBS. Protein aliquots, suspended in PBS, were stored at -20°C. In duplicate, 10 µL of BSA standards and cell protein samples were transferred to a clear 96-well microplate, followed by 200 µL of the Pierce BCA Protein Assay Kit working reagent in each well. The microplate was then incubated at 37°C for 30 minutes. Following incubation, the absorbance of each standard and sample was read at 560 nm using a Perkin Elmer Victor X5 2030 microplate reader. The protein content of each sample was quantified using a BSA standard curve (Figure 7) and used to normalize intracellular GSH, determined by the intracellular GSH assay.

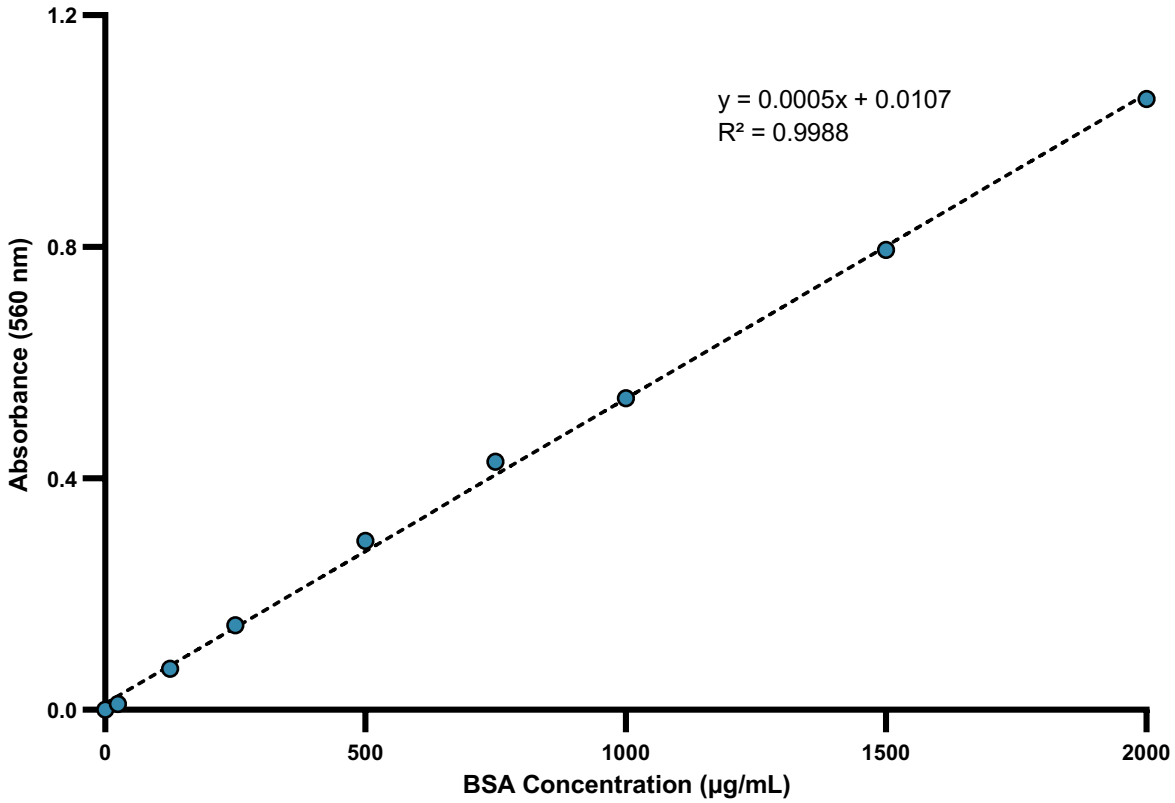

Figure 7. Standard curve of bovine serum albumin (BSA), used to normalize intracellular GSH values determined via the DTNB assay. Absorbance was read at 560 nm using a Perkin Elmer Victor X5 2030 microplate reader. Background absorbance was subtracted.

2.8 Data Analysis

Shapiro-Wilk and Kolmogorov-Smirnov tests were conducted to test for normality of technical replicates and biological replicates. Quantile-quantile (QQ) plots are provided (Appendix D). For experiments with technical replicates within biological replicates, a Nested One-Way ANOVA and Tukey Multiple Comparisons Test were conducted. For assays without technical replicates (i.e. the trypan blue exclusion assay), a One-Way ANOVA and Tukey Multiple Comparisons Test were conducted. All analyses were conducted using GraphPad Prism (Version 10.0).

3.0 Results

3.1.1 Effects of Chronic Iron and DFO on THP-1 Cell Metabolic Activity

To evaluate the effects of chronic exposure to iron excess and deficiency on metabolic activity, THP-1 cells were treated with varying doses of ferric citrate and DFO for 96 hours (Figure 8). THP-1 cells treated with either 10 µM, 20 µM, 40 µM, 100 µM, 150 µM, or 200 µM ferric citrate displayed no significant change in resorufin fluorescence, indicating no change in metabolic activity. These results show that THP-1 cell energetics were unaffected by chronic exposures to excess iron. Cells treated with 10 µM and 20 µM DFO experienced no significant change in metabolic activity, although there is notable variance in these conditions and the DFO control. Larger doses of DFO, however, induced significant reductions in THP-1 cell metabolic activity. 40 µM DFO induced a 60.7% reduction in metabolic activity, relative to control cells (+/- 34.4%, $p = 0.0082$), while 100 µM DFO induced a mean 91.2% reduction in metabolic activity, relative to control cells (+/- 4.7%, $p < 0.0001$). Thus, THP-1 cells are metabolically sensitive to chronic iron chelator treatments (40 µM and 100 µM DFO).

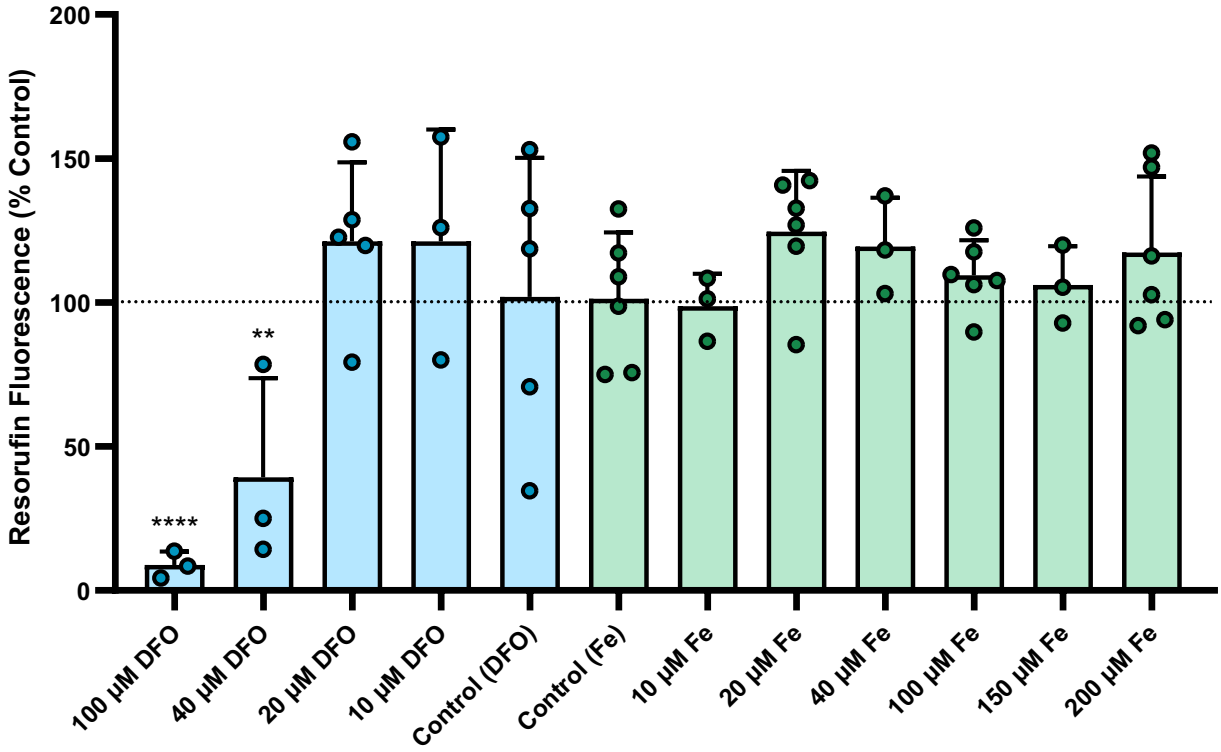

Figure 8. Mean metabolic activity of THP-1 cells after 96-hour treatments with ferric citrate (Fe) or DFO, determined by the resazurin metabolic assay (n = 3-6). Resorufin fluorescence was measured at 560 nm in a Perkin Elmer Victor X5 2030 microplate reader. Background fluorescence was subtracted from each value, which were then normalized to cell number. Fe-treated cells are shown in green, DFO-treated cells are shown in blue. Dots depict biological replicates. Error bars depict standard deviation. p = 0.0332 (*), p = 0.0021 (**), p = 0.0002 (***), p < 0.0001 (****).

3.1.2 Effects of Erastin on THP-1 Cell Metabolic Activity: Synergy with DFO

To examine the effects of erastin on THP-1 cells and probe for potential synergies with excess iron and DFO, cells treated with ferric citrate and DFO were administered 40 µM erastin after 72 hours of ferric citrate or DFO treatment elapsed (Figure 9). THP-1 cells treated solely with 40 µM erastin (i.e. control cells treated with erastin after 72 hours) displayed no significant change in resorufin fluorescence, relative to control cells. Cells co-treated with 40 µM erastin and ferric citrate (20 µM, 100 µM, 200 µM) displayed no significant change in resorufin fluorescence relative to control cells. This result indicates that the cells detected by the resazurin assay – that is, the cells that have not died as a result of their treatment conditions – are metabolically resistant to a large dose (40 µM) of erastin in iron-rich environments. THP-1 cells co-treated with 40 µM erastin and 20 µM DFO displayed a mean 53.2% reduction in metabolic output relative to control cells (+/- 11.4%, p = 0.0029), and a mean 60.5% reduction in metabolic output relative to cells treated solely with 20 µM DFO (p < 0.0001). Thus, in the cells that survived the cotreatment, 20 µM DFO synergized with 40 µM erastin to induce a significantly greater reduction in metabolic output than either treatment induced individually.

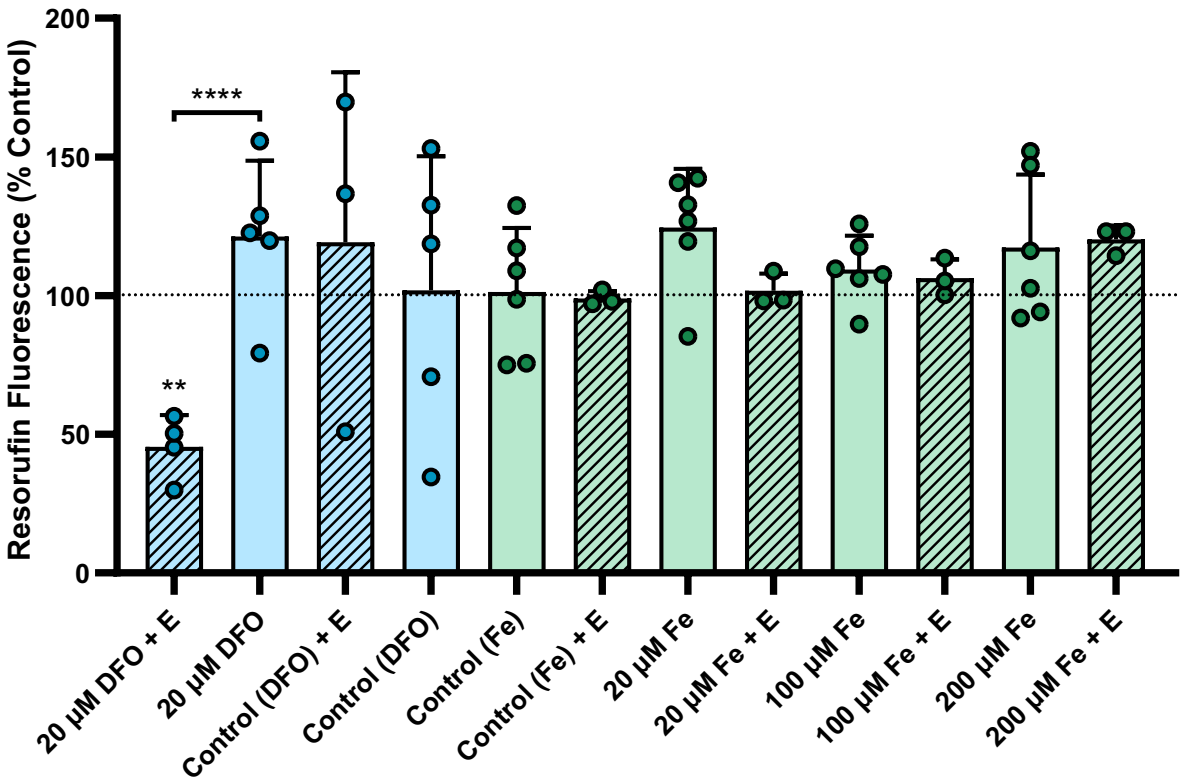

Figure 9. Mean metabolic activity of THP-1 cells after 96-hour treatments with ferric citrate (Fe) or DFO, with or without a 24-hour 40 µM erastin-treatment (E), determined by the resazurin metabolic assay (n = 3-6). Background fluorescence was subtracted from each value, which were then normalized to cell number. Fe-treated samples are depicted in green, DFO-treated samples are depicted in blue, erastin-treated samples are depicted by diagonal line pattern. Dots depict biological replicates. Error bars depict standard deviation. p = 0.0332 (*), p = 0.0021 (**), p = 0.0002 (***), p < 0.0001 (****).

3.2.1 Chronic Iron, DFO, and Erastin Cotreatment: THP-1 Cell Death

The lethality of chronic exposure to iron excess and deficiency, as well as erastin (co)treatment, was examined in THP-1 cells (Figure 10). As shown in Figure 10, THP-1 cell control samples had a mean viability of 94.2% (+/- 5.4%), that is, a mean death rate of 5.8%. Samples treated with 20 µM, 100 µM, and 200 µM ferric citrate showed negligible reduction in viability. Samples treated solely with 40 µM erastin had a mean viability of 79.3% (+/- 7.6%), indicating an average 3.6-fold increase in cell death relative to the control samples (p = 0.016). Samples co-treated with 20 µM ferric citrate and 40 µM erastin had a mean viability of 74.1% (+/- 11.5%, p = 0.0096), indicating an

average 5.6-fold increase in cell death resulting from erastin cotreatment, relative to samples treated solely with 20 μM ferric citrate ($p = 0.013$). Samples co-treated with 100 μM ferric citrate and 40 μM erastin had a mean viability of 66.9% (+/- 7.3%, $p < 0.00010$), indicating an average 4.4-fold increase in cell death resulting from erastin cotreatment, relative to samples treated solely with 100 μM ferric citrate ($p = 0.0012$). Samples co-treated with 200 μM ferric citrate and 40 μM erastin had a mean viability of 47.9% (+/- 8.0%, $p < 0.0001$), indicating an average 6.1-fold increase in cell death as a result of erastin cotreatment, relative to samples treated solely with 200 μM ferric citrate ($p < 0.0001$). Thus, erastin lethality in THP-1 cells is augmented by treatment with ferric citrate. This synergizing effect is most prominent in states of iron excess, as is shown in treatments with 200 μM ferric citrate.

THP-1 cell samples treated with 20 μM DFO had a mean viability of 49.3%, indicating an average 8.7-fold increase in cell death, relative to the control samples (+/- 15.9%, $p < 0.0001$). Samples treated with 20 μM DFO and 40 μM erastin had a mean viability of 15.5% (+/- 3.5%, $p < 0.0001$), indicating an average 5.1-fold increase in cell death relative to samples treated solely with 40 μM erastin ($p < 0.0001$) and an average 14.6-fold increase in cell death relative to control samples ($p < 0.0001$). 40 μM DFO and 100 μM DFO were similarly impactful, inducing average sample viabilities of 15.9% (+/- 0.8%, $p < 0.0001$) and 11.9% (+/- 3.4%, $p < 0.0001$), respectively. Thus, cotreatment of DFO and erastin synergistically induces mass THP-1 cell death, and larger doses of DFO (40 μM, 100 μM) are similarly lethal.

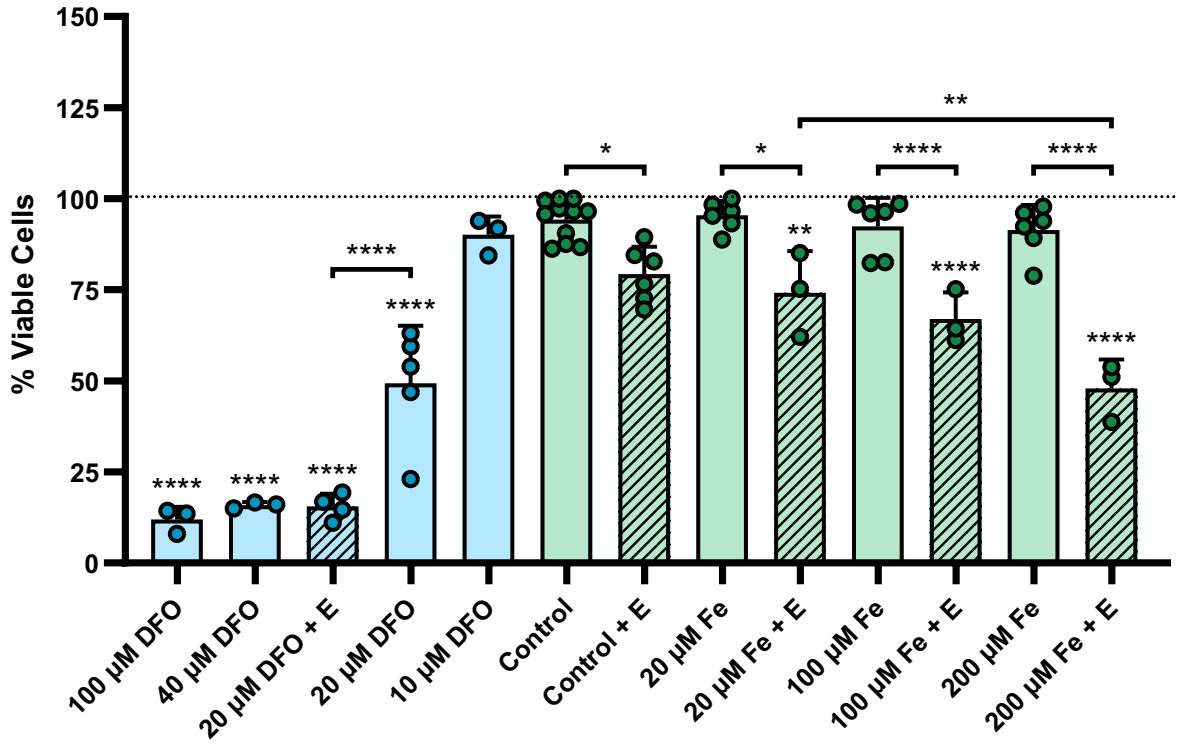

Figure 10. Mean sample viability of THP-1 cells after 96-hour treatments with ferric citrate (Fe) or DFO, with or without a 24-hour 40 µM erastin-treatment (E), determined by the trypan blue exclusion assay (n = 3-11). Fe-treated samples and control samples are depicted in green, DFO-treated samples are depicted in blue, erastin-treated samples are depicted by diagonal line pattern. Dots depict biological replicates. Error bars depict standard deviation. p = 0.0332 (*), p = 0.0021 (**), p = 0.0002 (***), p < 0.0001 (****).

3.2.2 THP-1 Cell Morphology Differs in Iron-Erastin and DFO-Erastin Cotreatments

THP-1 cell morphology was observed as a qualitative measure of the impacts of erastin cotreatments (Figure 11). Cells co-treated with 20 µM ferric citrate and 40 µM erastin showed little morphological changes (Figure 11B). Relative to control cells (Figure 11A), there was a greater quantity of dark cells and blebbing cells, suggesting an increase in sample disturbance and cell death. Cells co-treated with 200 µM ferric citrate and 40 µM erastin (Figure 11C) exhibited a marked increase in dark and blebbing cells, relative to control cells and to cells co-treated with 20 µM ferric citrate and 40 µM erastin. Cells treated with 20 µM DFO and 40 µM erastin (Figure 11D)

appeared the most disturbed of all co-treated samples, exhibiting a significant amount of cellular debris surrounding the cells. These cells were mostly dark and highly granular, indicating poor viability and marked cell death. There was far less blebbing than was observed in samples co-treated with 200 µM ferric citrate and 40 µM erastin, possibly suggesting an alternate form of cell death.

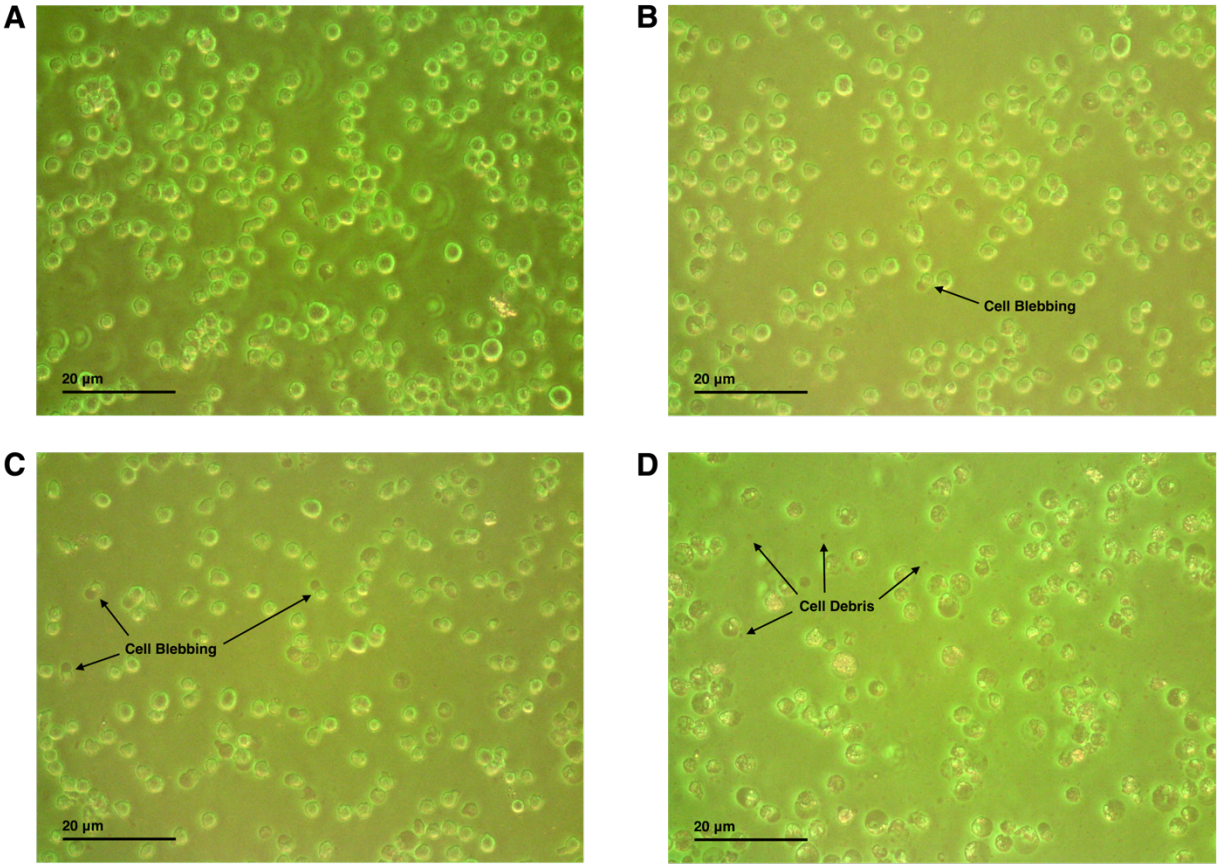

Figure 11. Photomicrographs of THP-1 cells after 96-hour treatments, taken using a Dino-Eye Eyepiece Camera and a Nikon Eclipse TS100 phase-contrast microscope. Cell blebbing and debris are pointed out. Scale bar represents 20 µm. **(A)** Control. **(B)** 20 µM ferric citrate and 40 µM erastin. **(C)** 200 µM ferric citrate and 40 µM erastin. **(D)** 20 µM DFO and 40 µM erastin.

3.3 Chronic Iron, DFO, and Erastin Cotreatment: THP-1 Cell GSH Response

To examine the importance of GSH and the GSH-GPX4 axis in THP-1 cells, intracellular GSH was measured after 96-hour treatments with ferric citrate and DFO, and erastin (co)treatments (Figure 12). THP-1 cells treated solely with 40 µM erastin

(i.e. control cells treated with erastin after 72 hours) displayed small reductions in intracellular GSH. Following treatment with erastin, iron control cells displayed a mean 13.4% reduction in GSH content (+/- 0.9%, non-significant), while DFO control cells experienced a mean 15.6% reduction in GSH content (+/- 7.3%, non-significant). Although statistically insignificant, we observed that THP-1 cells co-treated with ferric citrate and 40 µM erastin displayed a subtle, yet consistent iron-dose dependent reduction in intracellular GSH. Most notably, THP-1 cells treated with 200 µM ferric citrate and 40 µM erastin showed a mean 23.2% reduction in GSH content, relative to control cells (+/- 1.4%, non-significant), and a mean 17.9% reduction in GSH content relative to cells treated solely with 200 µM ferric citrate (non-significant). THP-1 cells treated with 20 µM DFO displayed a mean 17.1% reduction in GSH content, relative to control cells (+/- 6.8%, non-significant). Cells treated with 20 µM DFO and 40 µM erastin displayed a mean 19.0% increase in GSH content, relative to control cells (+/- 6.4%, non-significant), a mean 54.7% increase in GSH content relative to cells treated solely with 20 µM DFO ($p = 0.0068$), and a mean 54.9% increase in GSH content relative to cells treated solely with 40 µM erastin ($p = 0.012$).

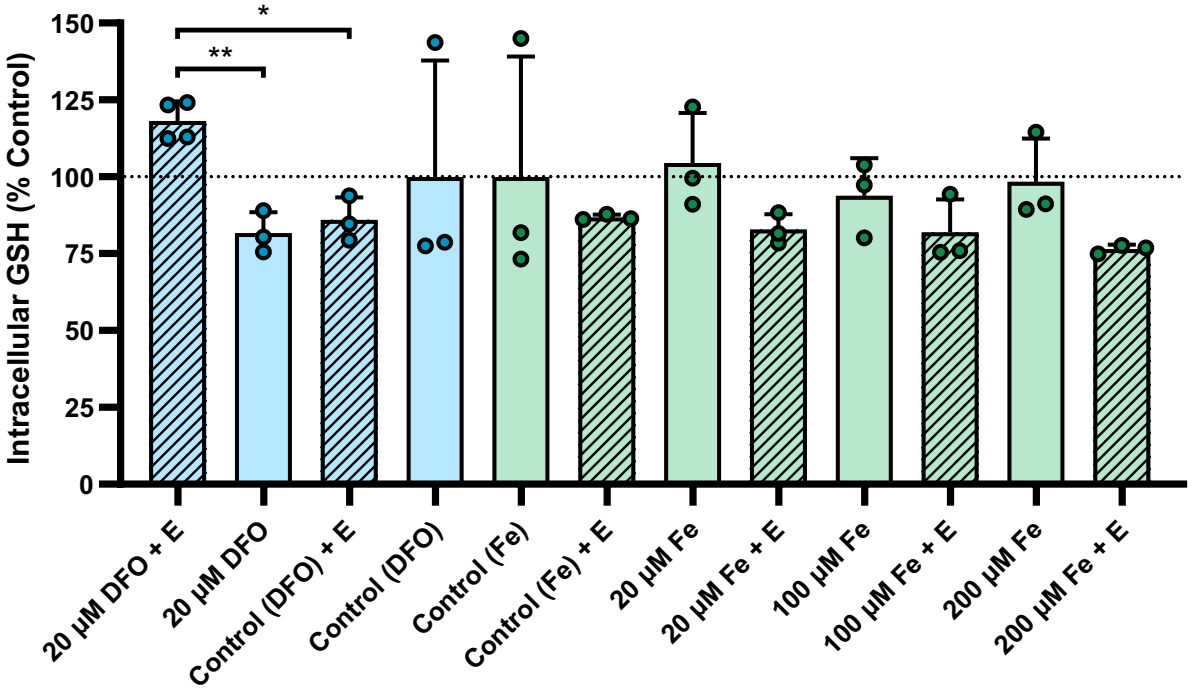

Figure 12. Mean intracellular GSH of THP-1 cells after 96-hour treatments with ferric citrate (Fe) or DFO, with or without a 24-hour 40 μM erastin-treatment (E), determined by the DTNB assay (n = 3-4). Fe-treated samples and control samples are depicted in green, DFO-treated samples are depicted in blue, erastin-treated samples are depicted by diagonal line pattern. Dots depict biological replicates. Error bars depict standard deviation. $p = 0.0332$ (*), $p = 0.0021$ (**), $p = 0.0002$ (***), $p < 0.0001$ (****).

4.0 Discussion

The present study sought to further examine the relationship of transformed monocytic (THP-1) cells with iron. Specifically, I sought to investigate the effects of chronic exposure to excess iron and DFO, and to probe for potential synergistic cotreatment with erastin. THP-1 cell viability and metabolic activity were, as hypothesized, unaffected by chronic exposure to excess iron. Unexpectedly, intracellular GSH levels were also unaltered by chronic exposure to excess iron, irrespective of dose. While cell death increased, surviving THP-1 cells were largely unaffected by erastin treatment, validating previous research and our hypotheses (Kumada et al., 2024; Ye et al., 2019; Yu et al., 2015). As was also hypothesized, THP-1 cell death increased in an iron dose-dependent manner when co-treated with erastin. Unexpectedly, the remaining viable cells co-treated with iron and erastin experienced no change in metabolic activity. Erastin did, however, ubiquitously induce a consistent yet small reduction in detectable intracellular GSH in control cells and iron-treated cells. As was hypothesized, moderate to high doses of DFO were very toxic in THP-1 cells, inducing significant cell death and reduced metabolic output. As was also expected, cotreatment with DFO and erastin proved devitalizing in THP-1 cells, inducing significant cell death and reduced metabolic output in those that survived their treatment. Surprisingly, however, intracellular GSH levels were the highest in cells co-treated with DFO and erastin.

4.1 THP-1 Cell Resistance to Excess Iron

The present study demonstrates that THP-1 cells are highly resistant to excess iron, as are other leukemic cell lines (Gharagozloo et al., 2008; Kraml et al., 2005;

Zheng et al., 2017). This marked resistance reflects the fact that, fundamentally, THP-1 cells are monocyte-macrophages. Aside from phagocytizing pathogens in response to infection, these cells engulf senescent erythrocytes and take up excess iron to facilitate iron recycling and avoid bacterial iron uptake (Hume, 2006). This physiological role necessitates an intrinsic capacity to cope with and store large iron quantities. THP-1 cells are known to express the iron-influx proteins TFR1 and TFR2, DMT1, ZIP8 and ZIP14 (Alluri et al., 2021; Egusa et al., 2023; Pandur et al., 2022; Qingmei et al., 2010; Reddy et al., 2012). ZIP14 is negatively regulated by p53 (Zhao et al., 2017), implying that THP-1 cells, which are p53 mutants, lack this downregulation. Being monocyte-macrophages, these cells also likely take up iron through CD163 and CD91 (Garcia et al., 2008; Maniecki et al., 2006), and possibly through the $beta_3$-integrin-IMP pathway, as is seen in other leukemic cells (Conrad et al., 1994). Furthermore, iron-loading with ferric citrate is shown to upregulate FT synthesis in THP-1 cells, indicating that they can increase iron storage in instances of iron excess (Risko et al., 2015).

Other cell types, even transformed cells, succumb to ferroptotic cell death in lower, shorter exposures to ferric citrate chelates (Wu et al., 2021). As such, THP-1 cells of the present study appeared to evade ferroptotic cell death in these chronic exposures to excess ferric citrate. This implies that THP-1 cells upregulate mechanisms crucial to the regulation of Fenton chemistry and repair of lipid peroxides in the plasma membrane, mitochondrial membranes and membrane of the ER (von Krusenstiern et al., 2023). Of these potential mechanisms, the GSH-GPX4 axis was hypothesized to be central in THP-1 cell survival in these conditions. In the present study, it was found that in states of chronic iron exposure, intracellular GSH levels were marginally reduced. While only the reduced form of GSH was measured (as opposed to the total pool, GSH + GSSG), this suggests two plausible mechanisms: first, that THP-1 cells were synthesizing GSH and regenerating GSH from GSSG (via glutathione reductase) at a similar rate to its expenditure. In stressful conditions, p53 is known to negatively regulate the expression of system x_C^-, reducing the uptake of cysteine, the limiting amino acid of GSH synthesis (Jiang et al., 2015). THP-1 cells, then, lack this

downregulation, facilitating sufficient system x_C^- expression for rapid GSH synthesis. Second, this could suggest that THP-1 cells rely on alternative mechanisms to sequester ROS and repair lipid peroxides, like FSP1. THP-1 cells are known to express catalase, a ROS-scavenger that requires iron for its heme-containing active site (Alfonso-Prieto et al., 2009; Hervé-Grépinet et al., 2008). Storing excess iron can further combat the propensity for iron-catalyzed ROS formation (Hou et al., 2016), and in the present study, THP-1 cells may have heightened FT production to retain more iron in a redox-inactive form.

THP-1 cells have homozygous deletions of p15, p16, p73, and a 26-codon deletion of p53 (Adati et al., 2009; Sugimoto et al., 1992). In combination, these mutations permit unrestrained cell cycle progression, irrespective of DNA damage signals (Foulkes et al., 1997; Levrero et al., 2000; Marei et al., 2021; Xia et al., 2021). Additionally, THP-1 cells have homozygous PTEN deletions, allowing for dysregulated PI3K-PKB activation (Adati et al., 2009). PKB activation has implications in cell death through the inhibition of *Bad*, a protein that negatively regulates antiapoptotic proteins *B-cell lymphoma 2* (BCL-2) and *B-cell lymphoma XL* (BCL-XL) (Hopkins et al., 2014). In the presence of excess iron, ROS production in THP-1 cells presumably increases, increasing the likelihood of genetic aberration – without these cell cycle regulators, THP-1 cells would fail to respond to DNA damage signals and continue to proliferate.

4.2 THP-1 Cell Resistance to Erastin: Attenuated by Excess Iron?

The present study validated that THP-1 cells are only mildly affected by a high dose (40 µM) of erastin, as are various leukemic cell lines (Kumada et al., 2024; Ye et al., 2019; Yu et al., 2015). In an effort to further examine this phenomenon in the presence of excess iron and elucidate the role of the GSH-GPX4 axis in THP-1 cells, erastin was administered to cells in varying concentrations of excess NTBI. When co-treated with erastin, THP-1 cell death increased in an iron dose-dependent manner. Notably, THP-1 cell metabolic output was unaffected in any of the iron-erastin cotreatments. This discrepancy between live:dead ratios and metabolic activity is likely

a result of the resazurin assay only measuring viable, metabolically active cells. Cells that died as a result of their treatment are largely excluded from the assay through centrifugation and media resuspension, and those that remain are simply not detected. This suggests the presence of cells with differing degrees of fitness within the cultured samples. Indeed, the administration of erastin and excess iron poses a selective pressure. Cultured cancer cells (i.e. *in-vitro*), as observed *in-vivo*, harbor mutational heterogeneity that correlates to their relative success within the cell population (Bowling et al., 2019; Esparza-López et al., 2016).

Without examining the mode of death, I assume that the increased rate of cell death in the iron-erastin co-treatments is the result of ferroptosis. Interestingly, intracellular GSH levels were reduced by no more than 23% (200 μM ferric citrate and 40 μM erastin; Figure 12) by co-treatments of ferric citrate and erastin. This suggests that alternative mechanisms of ROS sequestration and lipid peroxide repair, like catalase and FSP1 activity, are employed in THP-1 cells. Alternatively, cancer cells are known to acquire nutrients via pinocytosis and entosis – modes of endocytosis in which extracellular proteins and necrotic cell debris are absorbed through an invagination of the plasma membrane and degraded for usage in the cell (Pavlova et al., 2022). In a recent study, multiple transformed cell types were shown to evade cysteine depletion-induced ferroptosis by pinocytotically absorbing extracellular cysteine in the form of albumin, an abundant, cysteine-rich protein in circulation (Armenta et al., 2022). One of the principal proteins in FBS, and in most common cell culture media, is bovine serum albumin (Lee et al., 2023). Considering the intrinsic phagocytic capability of monocyte-macrophages, this makes for a compelling possibility: THP-1 cells of the present study may have acquired cysteine for GSH biosynthesis from the culture media through the pinocytotic absorption of BSA, contributing to their marked erastin resistance. In states of iron excess, this potential mechanism for the uptake of cysteine may have fostered cell competition within samples, a general phenomenon that occurs in-vivo and selects for ‘super-fit’ cancer cells (Bowling et al., 2019). In the present study, THP-1 cells were treated with erastin 24 hours after their mid-treatment (48-hour) media refresh, at which

point the cell density was often 2- or 3-fold greater than their initial density. Nutrients may have been very limited by that stage, especially with such high confluence. This could have contributed to the possibility of natural selection occurring within samples. As for the cells that died, elevated iron-catalyzed oxidative stress is presumed to be responsible: more redox-active iron is cycled through Fenton-Haber-Weiss reactions, producing more (lipid) ROS and subsequently, demanding a greater antioxidant response (Yan et al., 2021). Erastin treatment renders GSH biosynthesis more arduous and these cells likely struggled to maintain an adequate pace of lipid peroxide repair, one of the hallmarks of ferroptosis (Dixon & Stockwell, 2019).

4.3.1 DFO Toxicity in THP-1 Cells

The present study validates previous findings of THP-1 cell sensitivity to DFO and in comparison, demonstrates that chronic exposures extend the lethality of DFO (Neumannova et al., 1995; Seo et al., 2006). Unsurprisingly, DFO-treated THP-1 cells of the present study appeared highly distressed, as evidenced by a reduction in confluence and cell size, increased surrounding cellular debris, cell blebbing, dark granular appearance and increased adherence to culture plates. DFO can induce the differentiation of THP-1 cells to functional macrophages, supporting the observation of increased cell adherence in the present study (Seo et al., 2006). Empirically, THP-1 cells subjected to chronic treatment with 40 µM and 100 µM DFO experienced devastating cell death and a significant reduction in metabolic activity. DFO induces cell cycle arrest through LIP depletion and subsequent inability to synthesize deoxyribonucleotides via RNR (Cooper et al., 1996; Furukawa et al., 1992), likely contributing to the observed DFO toxicity. In acute doses, DFO can sequester excess iron to rescue cells from the accumulation of ROS and subsequent induction of ferroptosis, while longer treatments and larger doses of DFO can increase mROS production by inducing ETC dysfunction (Zhang et al., 2019; Zhang et al., 2020). Without sufficient cellular iron, ETC complexes I, II, III and IV are less, if at all, capable of shuttling electrons (Xu et al., 2013). In an aerobic environment, this means that O_2 can no longer be fully reduced to H_2O, resulting in the production of partially reduced

oxygen species like $O_2^{\bullet-}$ and H_2O_2 (Lenaz, 2012). Fittingly, intracellular GSH levels were decreased in THP-1 cells treated with 20 μM DFO, indicating an increased demand and utilization for the antioxidant reduction of ROS. This suggests that the toxicity observed in this study, both empirically and morphologically, is a result of mitochondrial dysfunction and elevated mROS production.

While the observed mode of death can only be speculated, it is presumed that most DFO-treated THP-1 cells underwent a form of apoptosis, because in other leukemic and myelomic cell lines, DFO treatment induces apoptosis (Liu & Zhu, 2022; Yang et al., 2021; Yang et al., 2018). These studies document an increase in ROS production, reduced expression of antiapoptotic proteins BCL-2 and BCL-XL, as well as heightened expression of pro-apoptotic protein Bax. As further evidence that apoptosis is the probable mode of DFO-induced cell death, DFO is known to increase activation of the mitogen-activated protein kinase (MAPK) apoptotic pathway and heighten expression of caspases 3 and 9, proteases ubiquitously responsible for a cell's intrinsic induction of apoptosis (Kim et al., 2016; Xue et al., 2021).

4.3.2 Erastin-DFO Synergy

While DFO is known to have potent antileukemic potential on its own, published findings have demonstrated synergistic DFO cotreatments with chemotherapy agents (Leardi et al., 2001; Yalcintepe & Halis, 2016). Co-treating leukemic cells with DFO and erastin, however, has not previously been explored. The present study demonstrates that in THP-1 cells, a moderate dose of DFO (20 μM) synergizes with erastin (40 μM), inflicting a 5-fold increase in cell death relative to cells treated solely with erastin. Unexpectedly, GSH levels were notably elevated in this treatment condition, relative to all other treatment conditions. Without measuring the relative levels of GSH and GSSG, though, one cannot conclude that these cells simply were not utilizing GSH. Considering the prevailing evidence that DFO and erastin heighten the presence of ROS and reduce GSH levels on their own, it would seem counterintuitive for THP-1 cells to lessen their expenditure of GSH (Liu & Zhu, 2022; Sato et al., 2018; Seo et al., 2006). Rather, it may

be that in response to such a stressful cotreatment, GSH biosynthesis is swiftly upregulated – as previously observed (Lu, 2009, 2013; Soeur et al., 2015). While the cells were likely to be using GSH to sequester ROS, the total GSH pool (GSH + GSSG) may have elevated in response to this treatment, resulting in the subsequent detection of heightened intracellular GSH. Furthermore, the DTNB assay is mainly measuring the contents of living cells since the dead cells, which are less dense, are largely eradicated through the washing step of the assay protocol. As such, the remaining 15% of cells that are viable are likely to have prevailed because they boosted their antioxidant response.

Aside from blocking system x_C^-, erastin diffuses across the plasma membrane and interacts with voltage-dependent anion channels (VDACs) on the OMM (Maldonado et al., 2013). VDACs are metabolite channels with a preference for anionic species, most notably ATP, chloride (Cl^-), glutamate, phosphate, and various ROS (Heslop et al., 2021). Accounting for 10% of OMM proteins, VDACs are abundant and vital to mitochondrial metabolite flux, membrane potential, and apoptosis (Mazure, 2017). Tubulin, a cytoskeletal protein of greater abundance in transformed cells, acts as a VDAC blocker and has implications in cancer metabolism by reducing the efflux of ATP and the influx of adenosine diphosphate (ADP) (and P_i), facilitating a more glycolytic metabolic balance (Maldonado, 2017). Pivotally, erastin competes with tubulin and reverses tubulin VDAC blockage, thereby permitting the VDAC open conformation (Maldonado et al., 2013). This results in a cascade of changes: VDAC conductance increases, inducing anionic metabolite flow into the intermembrane space (IMS), hyperpolarizing the mitochondrial membrane. Among various implications, this eliminates the proton-motive force required for ATP synthesis and in combination, these changes are very stressful on mitochondrial homeostasis (DeHart et al., 2018; Mazure, 2017; Y. Zhao et al., 2020).

VDACs are linked to apoptosis in a number of ways. Cytochrome C, released from the mitochondria to induce the intrinsic apoptotic pathway, can flow through VDACs (Shimizu et al., 2001). Moreover, BCL-XL promotes the VDAC closed

conformation to prevent apoptosis, while Bax and Bak directly enhance the activity of VDACs (Mazure, 2017). Most notably, Bax are shown to interact with VDACs and form a novel channel, approximately 4- and 10-fold larger than VDAC and Bax channels, respectively (Shimizu et al., 2000). This process allows for expedited cytochrome C release and induction of apoptosis. As was previously described, abundant research supports the pro-apoptotic action of DFO in leukemic cells, evidenced by iron-deprived mitochondrial dysfunction, heightened expression of Bax/Bak and effector caspases, and lessened expression of BCL-2/XL. In combination, the aforementioned mechanisms of DFO and erastin are decidedly lethal and effective at largely eradicating THP-1 cells. The findings of the present study suggest that combining iron chelators like DFO with erastin analogues pose as novel avenues for antileukemic research and therapy.

4.4 Limitations

There were several limitations to the present study. The resazurin metabolic assay measures active metabolism, meaning that only cells that survived their treatment were assessed. In the more lethal treatment conditions, then, this assay only measured a small, robust subset of cells in these samples. Moreover, the lethality of 40 µM and 100 µM DFO, as well as the DFO-erastin cotreatment, resulted in very few remaining viable cells by the end of their 96-hour treatment. Subsequently, as few as approximately 3,600 DFO-treated cells were measured by the resazurin metabolic assay. At such a low cell density, fluorescence measures can be close to their detection limit and thus highly variable, as they often were in this study. Ideally, resorufin fluorescence of a higher cell density would be measured for the DFO treatment conditions. To further combat variability in fluorescence, it would be ideal to normalize resorufin fluorescence to protein samples, as opposed to cell number. Resorufin fluorescence could equally be measured using flow cytometry, for even greater precision. The present study measured intracellular GSH and did not quantify its oxidized counterpart, GSSG. In order to conclusively determine the GSH antioxidant response to all the treatment conditions, measuring the GSH:GSSG ratio is imperative. THP-1 cells reside in suspension, requiring centrifugation to refresh treatments and

media, and to dilute samples to desired densities for measurement. In doing so, dead and dying cells are largely eradicated from the sample, meaning that the measured intracellular GSH levels were predominantly of the surviving, more robust cells. Lastly, the erastin treatments were administered after 72 hours of unimpeded growth, at which point the iron-treated cells and control cells were highly confluent. Overconfluence can trigger cell death on its own, so the observed effects of erastin may have been amplified by an over-crowding effect.

4.5 Future Directions

It would be of value to investigate mode of death in erastin cotreatments with DFO and iron, as would the investigation of ROS production in response to these treatments. Future studies can investigate the role of erastin-regulated VDACs in THP-1 cells, as well as the activity of apoptotic proteins like Bax, BCL-2, and cytochrome C. Furthermore, it would be of interest to examine the potential for pinocytotic acquisition of nutrients like cysteine and its link to THP-1 cell erastin resistance. Finally, it would be of interest to examine alterative antiferroptotic mechanisms, beyond the GSH-GPX4 axis.

5.0 Conclusions

Results of the present study demonstrate that THP-1 cells are very robust in chronic states of iron excess, while highly sensitive to iron deprivation through chronic DFO treatment. This study validates previous reports of THP-1 cell resistance to erastin and suggests that THP-1 cells are using alternate methods of cysteine acquisition (other than system x_C^-) and lipid peroxide repair (other than GPX4), although our results indicate that ferric citrate attenuates THP-1 cell erastin resistance. Most notably, this study exhibits novel evidence of a synergistic lethality between DFO and erastin. This result suggests a novel avenue of research and antileukemic combination therapy of an iron chelator with a ferroptosis-inducing compound like erastin.

References

Abbaspour, N., Hurrell, R., & Kelishadi, R. (2014). Review on iron and its importance for human health. *Journal of Research in Medical Sciences: The Official Journal of Isfahan University of Medical Sciences*, *19*(2), 164. /pmc/articles/PMC3999603/

Åbrink, M., Gobl, A. E., Huang, R., Nilsson, K., & Hellman, L. (1994). Human cell lines U-937, THP-1 and Mono Mac 6 represent relatively immature cells of the monocyte-macrophage cell lineage. *Leukemia*, *8*(9), 1579–1584. https://europepmc.org/article/med/8090034

Adati, N., Huang, M. C., Suzuki, T., Suzuki, H., & Kojima, T. (2009). High-resolution analysis of aberrant regions in autosomal chromosomes in human leukemia THP-1 cell line. *BMC Research Notes*, *2*, 153. https://doi.org/10.1186/1756-0500-2-153

Alfonso-Prieto, M., Biarnés, X., Vidossich, P., & Rovira, C. (2009). The molecular mechanism of the catalase reaction. *Journal of the American Chemical Society*, *131*(33), 11751–11761. https://doi.org/10.1021/JA9018572/SUPPL_FILE/JA9018572_SI_001.PDF

Alluri, K., Yathapu, S. R., Babu Kondapalli, N., Hemalatha, R., Nair, K. M., & Ghosh, S. (2021). Levels of zinc transporters mRNA depending on zinc status and HIV-1 tat induced inflammation in muscle (rhabdomyosarcoma) and monocyte (THP-1) cell lines. *Biochemistry (Moscow)*, *86*(2), 168–178. https://doi.org/10.1134/S000629792102005X/FIGURES/7

Armenta, D. A., Laqtom, N. N., Alchemy, G., Dong, W., Morrow, D., Poltorack, C. D., Nathanson, D. A., Abu-Remalieh, M., & Dixon, S. J. (2022). Ferroptosis inhibition by lysosome-dependent catabolism of extracellular protein. *Cell Chemical Biology*, *29*(11), 1588-1600.e7. https://doi.org/10.1016/j.chembiol.2022.10.006

Armstrong, N., Ryder, S., Forbes, C., Ross, J., & Quek, R. G. W. (2019). A systematic review of the international prevalence of BRCA mutation in breast cancer. *Clinical Epidemiology*, *11*, 543–561. https://doi.org/10.2147/CLEP.S206949

Bartels, H., & Baumann, R. (1998). Respiratory function of hemoglobin. *New England Journal of Medicine*, *14*, 107–134. https://doi.org/10.1056/NEJM199801223380407

Basak, T., & Kanwar, R. K. (2022). Iron imbalance in cancer: Intersection of deficiency and overload. *Cancer Medicine*, *11*(20), 3837–3853. https://doi.org/10.1002/CAM4.4761

Bersuker, K., Hendricks, J. M., Li, Z., Magtanong, L., Ford, B., Tang, P. H., Roberts, M. A., Tong, B., Maimone, T. J., Zoncu, R., Bassik, M. C., Nomura, D. K., Dixon, S. J.,

& Olzmann, J. A. (2019). The CoQ oxidoreductase FSP1 acts parallel to GPX4 to inhibit ferroptosis. *Nature*, *575*(7784), 688–692. https://doi.org/10.1038/s41586-019-1705-2

Bertoli, S., Paubelle, E., Bérard, E., Saland, E., Thomas, X., Tavitian, S., Larcher, M. V., Vergez, F., Delabesse, E., Sarry, A., Huguet, F., Larrue, C., Bosc, C., Farge, T., Sarry, J. E., Michallet, M., & Récher, C. (2019). Ferritin heavy/light chain (FTH1/FTL) expression, serum ferritin levels, and their functional as well as prognostic roles in acute myeloid leukemia. *European Journal of Haematology*, *102*(2), 131–142. https://doi.org/10.1111/EJH.13183

Bogdan, A. R., Miyazawa, M., Hashimoto, K., & Tsuji, Y. (2016). Regulators of iron homeostasis: New players in metabolism, cell death, and disease. *Trends in Biochemical Sciences*, *41*(3), 274–286. https://doi.org/10.1016/j.tibs.2015.11.012

Bowling, S., Lawlor, K., & Rodríguez, T. A. (2019). Cell competition: The winners and losers of fitness selection. *Development (Cambridge)*, *146*(13). https://doi.org/10.1242/DEV.167486/19785

Bridges, R. J., Natale, N. R., & Patel, S. A. (2012). System xc- cystine/glutamate antiporter: an update on molecular pharmacology and roles within the CNS. *British Journal of Pharmacology*, *165*(1), 20–34. https://doi.org/10.1111/J.1476-5381.2011.01480.X

Brown, R. A. M., Richardson, K. L., Kabir, T. D., Trinder, D., Ganss, R., & Leedman, P. J. (2020). Altered iron metabolism and impact in cancer biology, metastasis, and immunology. *Frontiers in Oncology*, *10*, 533570. https://doi.org/10.3389/FONC.2020.00476/BIBTEX

Cancer. (2022, February 3). World Health Organization. https://www.who.int/news-room/fact-sheets/detail/cancer

Cancer statistics at a glance. (n.d.). Canadian Cancer Society. Retrieved June 14, 2023, from https://cancer.ca/en/research/cancer-statistics/cancer-statistics-at-a-glance?gclid=EAIaIQobChMIiInz0dTF_wIVDCWtBh1x3AkgEAAYASAAEgIvifD_BwE

Cardona, C. J., & Montgomery, M. R. (2023). Iron regulatory proteins: players or pawns in ferroptosis and cancer? *Frontiers in Molecular Biosciences*, *10*, 1229710. https://doi.org/10.3389/FMOLB.2023.1229710/BIBTEX

Combs, J. A., & Denicola, G. M. (2019). The non-essential amino acid cysteine becomes essential for tumor proliferation and survival. *Cancers*, *11*(5). https://doi.org/10.3390/CANCERS11050678

Conrad, M. E., Umbreit, J. N., Moore, E. G., Hainsworth, L. N., Porubcin, M., Simovich, M. J., Nakada, M. T., Dolan, K., & Garrick, M. D. (2000). Separate pathways for cellular uptake of ferric and ferrous iron. *American Journal of Physiology - Gastrointestinal and Liver Physiology*, *279*(4 42-4). https://doi.org/10.1152/AJPGI.2000.279.4.G767/ASSET/IMAGES/LARGE/H31000125007.JPEG

Conrad, M. E., Umbreit, J. N., Moore, E. G., Uzel, C., & Berry, M. R. (1994). Alternate iron transport pathway: Mobilferrin and integrin in K562 cells. *Journal of Biological Chemistry*, *269*(10), 7169–7173. https://doi.org/10.1016/s0021-9258(17)37263-0

Conrad, M., & Friedmann Angeli, J. P. (2015). Glutathione peroxidase 4 (Gpx4) and ferroptosis: What's so special about it? *Molecular & Cellular Oncology*, *2*(3). https://doi.org/10.4161/23723556.2014.995047

Cooper, C. E., Lynagh, G. R., Hoyes, K. P., Hider, R. C., Cammack, R., & Porter, J. B. (1996). The relationship of intracellular iron chelation to the inhibition and regeneration of human ribonucleotide reductase. *Journal of Biological Chemistry*, *271*(34), 20291–20299. https://doi.org/10.1074/jbc.271.34.20291

DeHart, D. N., Fang, D., Heslop, K., Li, L., Lemasters, J. J., & Maldonado, E. N. (2018). Opening of voltage dependent anion channels promotes reactive oxygen species generation, mitochondrial dysfunction and cell death in cancer cells. *Biochemical Pharmacology*, *148*, 155–162. https://doi.org/10.1016/J.BCP.2017.12.022

Dixon, S. J., Lemberg, K. M., Lamprecht, M. R., Skouta, R., Zaitsev, E. M., Gleason, C. E., Patel, D. N., Bauer, A. J., Cantley, A. M., Yang, W. S., Morrison, B., & Stockwell, B. R. (2012). Ferroptosis: An iron-dependent form of nonapoptotic cell death. *Cell*, *149*(5), 1060–1072. https://doi.org/10.1016/j.cell.2012.03.042

Dixon, S. J., & Olzmann, J. A. (2024). The cell biology of ferroptosis. *Nature Reviews Molecular Cell Biology 2024*, 1–19. https://doi.org/10.1038/s41580-024-00703-5

Dixon, S. J., & Stockwell, B. R. (2019). The hallmarks of ferroptosis. *Annual Reviews in Cancer Biology*, *3*(1), 35–54. https://doi.org/10.1146/ANNUREV-CANCERBIO-030518-055844

Doll, S., Freitas, F. P., Shah, R., Aldrovandi, M., da Silva, M. C., Ingold, I., Grocin, A. G., Xavier da Silva, T. N., Panzilius, E., Scheel, C. H., Mourão, A., Buday, K., Sato, M.,

Wanninger, J., Vignane, T., Mohana, V., Rehberg, M., Flatley, A., Schepers, A., … Conrad, M. (2019). FSP1 is a glutathione-independent ferroptosis suppressor. *Nature*, *575*(7784), 693–698. https://doi.org/10.1038/s41586-019-1707-0

Doll, S., Proneth, B., Tyurina, Y. Y., Panzilius, E., Kobayashi, S., Ingold, I., Irmler, M., Beckers, J., Aichler, M., Walch, A., Prokisch, H., Trümbach, D., Mao, G., Qu, F., Bayir, H., Füllekrug, J., Scheel, C. H., Wurst, W., Schick, J. A., … Conrad, M. (2016). ACSL4 dictates ferroptosis sensitivity by shaping cellular lipid composition. *Nature Chemical Biology*, *13*(1), 91–98. https://doi.org/10.1038/nchembio.2239

Dong, Y., Shi, O., Zeng, Q., Lu, X., Wang, W., Li, Y., Wang, Q., Wang, Q., & Wang, Q. (2020). Leukemia incidence trends at the global, regional, and national level between 1990 and 2017. *Experimental Hematology and Oncology*, *9*(1), 1–11. https://doi.org/10.1186/S40164-020-00170-6/FIGURES/5

Dutt, S., Hamza, I., & Bartnikas, T. B. (2022). Molecular mechanisms of iron and heme metabolism. *Annual Reviews in Nutrition*, *42*, 311–335. https://doi.org/10.1146/ANNUREV-NUTR-062320-112625

Egusa, K., Shibutani, S., & Iwata, H. (2023). IgG and insulin enhance endocytosis in THP-1 cells via activation of phosphatidylinositol 3-kinase (PI3K). *Biochemical and Biophysical Research Communications*, *679*, 160–166. https://doi.org/10.1016/J.BBRC.2023.09.008

Esparza-López, J., Ramos-Elías, P. A., Castro-Sánchez, A., Rocha-Zavaleta, L., Escobar-Arriaga, E., Zentella-Dehesa, A., León-Rodríguez, E., Medina-Franco, H., & Ibarra-Sánchez, M. de J. (2016). Primary breast cancer cell culture yields intra-tumor heterogeneous subpopulations expressing exclusive patterns of receptor tyrosine kinases. *BMC Cancer*, *16*(1), 1–14. https://doi.org/10.1186/S12885-016-2769-0/FIGURES/7

Estrov, Z., Tawa, A., Wang, X. H., Dubé, I. D., Sulh, H., Cohen, A., Gelfand, E. W., & Freedman, M. H. (1987). In vitro and in vivo effects of deferoxamine in neonatal acute leukemia. *Blood*, *69*(3), 757–761. https://doi.org/10.1182/BLOOD.V69.3.757.757

Finkel, T. (2011). Signal transduction by reactive oxygen species. *Journal of Cell Biology*, *194*(1), 7–15. https://doi.org/10.1083/JCB.201102095

Fonseca-Nunes, A., Jakszyn, P., & Agudo, A. (2014). Iron and cancer risk-a systematic review and meta-analysis of the epidemiological evidence. *Cancer Epidemiology Biomarkers and Prevention*, *23*(1), 12–31. https://doi.org/10.1158/1055-9965.EPI-

13-0733/67737/AM/IRON-AND-CANCER-RISK-A-SYSTEMATIC-REVIEW-AND-META

Fontham, E. T. H., Thun, M. J., Ward, E., Balch, A. J., John, ;, Delancey, O. L., & Samet, J. M. (2009). American Cancer Society Perspectives on Environmental Factors and Cancer. *CA: A Cancer Journal for Clinicians*, *59*(6), 343–351. https://doi.org/10.3322/CAAC.20041

Forman, H. J., Maiorino, M., & Ursini, F. (2010). Signaling functions of reactive oxygen species. *Biochemistry*, *49*(5), 835–842. https://doi.org/10.1021/BI9020378/ASSET/IMAGES/MEDIUM/BI-2009-020378_0001.GIF

Förstermann, U., & Sessa, W. C. (2012). Nitric oxide synthases: regulation and function. *European Heart Journal*, *33*(7), 829. https://doi.org/10.1093/EURHEARTJ/EHR304

Foulkes, W. D., Flanders, T. Y., Pollock, P. M., & Hayward, N. K. (1997). The CDKN2A (p16) gene and human cancer. *Molecular Medicine*, *3*(1), 5–20. https://doi.org/10.1007/BF03401664/TABLES/2

Fu, D., & Richardson, D. R. (2007). Iron chelation and regulation of the cell cycle: 2 mechanisms of posttranscriptional regulation of the universal cyclin-dependent kinase inhibitor p21CIP1/WAF1 by iron depletion. *Blood*, *110*(2), 752–761. https://doi.org/10.1182/BLOOD-2007-03-076737

Furukawa, T., Naitoh, Y., Kohno, H., Tokunaga, R., & Taketani, S. (1992). Iron deprivation decreases ribonucleotide reductase activity and DNA synthesis. *Life Sciences*, *50*(26), 2059–2065. https://doi.org/10.1016/0024-3205(92)90572-7

Ganz, T. (2013). Systemic iron homeostasis. *Physiological Reviews*, *93*(4), 1721–1741. https://doi.org/10.1152/PHYSREV.00008.2013/ASSET/IMAGES/LARGE/Z9J00413 26710006.JPEG

Gao, M., Monian, P., Quadri, N., Ramasamy, R., & Jiang, X. (2015). Glutaminolysis and transferrin regulate ferroptosis. *Molecular Cell*, *59*(2), 298–308. https://doi.org/10.1016/J.MOLCEL.2015.06.011

Garcia, C., Gardner, D., & Reichard, K. K. (2008). CD163: A specific immunohistochemical marker for acute myeloid leukemia with monocytic differentiation. *Applied Immunohistochemistry and Molecular Morphology*, *16*(5), 417–421. https://doi.org/10.1097/PAI.0B013E31815DB477

Gharagozloo, M., Khoshdel, Z., & Amirghofran, Z. (2008). The effect of an iron (III) chelator, silybin, on the proliferation and cell cycle of Jurkat cells: A comparison

with desferrioxamine. *European Journal of Pharmacology*, *589*(1–3), 1–7. https://doi.org/10.1016/J.EJPHAR.2008.03.059

Ginhoux, F., & Jung, S. (2014). Monocytes and macrophages: developmental pathways and tissue homeostasis. *Nature Reviews Immunology*, *14*(6), 392–404. https://doi.org/10.1038/nri3671

Guerinot, M. Lou. (2000). The ZIP family of metal transporters. *Biochimica et Biophysica Acta (BBA) - Biomembranes*, *1465*(1–2), 190–198. https://doi.org/10.1016/S0005-2736(00)00138-3

Guo, Q., Li, L., Hou, S., Yuan, Z., Li, C., Zhang, W., Zheng, L., & Li, X. (2021). The role of iron in cancer progression. *Frontiers in Oncology*, *11*, 778492. https://doi.org/10.3389/FONC.2021.778492/BIBTEX

Hagag, A. A., Badraia, I. M., Abdelmageed, M. M., Hablas, N. M., Hazzaa, S. M. E., & Nosair, N. A. (2018). Prognostic value of transferrin receptor-1 (CD71) expression in acute lymphoblastic leukemia. *Endocrine, Metabolic & Immune Disorders - Drug Targets*, *18*(6), 610–617. https://doi.org/10.2174/1871530318666180605094706

Hallek, M. (2017). Chronic lymphocytic leukemia: 2017 update on diagnosis, risk stratification, and treatment. *American Journal of Hematology*, *92*(9), 946–965. https://doi.org/10.1002/AJH.24826

Hanahan, D., & Weinberg, R. A. (2000). The hallmarks of cancer. *Cell*, *100*(1), 57–70. https://doi.org/10.1016/S0092-8674(00)81683-9

Hanahan, D., & Weinberg, R. A. (2011). Hallmarks of cancer: The next generation. *Cell*, *144*(5), 646–674. https://doi.org/10.1016/J.CELL.2011.02.013/ATTACHMENT/68024D79-3A9C-46C4-930B-640934F11E2E/MMC1.PDF

Hatcher, H. C., Singh, R. N., Torti, F. M., & Torti, S. V. (2009). Synthetic and natural iron chelators: Therapeutic potential and clinical use. *Future Medicinal Chemistry*, *1*(9), 1643–1670. https://doi.org/10.4155/FMC.09.121

Hervé-Grépinet, V., Veillard, F., Godat, E., Heuzé-Vourc'h, N., Lecaille, F., & Lalmanach, G. (2008). Extracellular catalase activity protects cysteine cathepsins from inactivation by hydrogen peroxide. *FEBS Letters*, *582*(9), 1307–1312. https://doi.org/10.1016/J.FEBSLET.2008.03.007

Heslop, K. A., Milesi, V., & Maldonado, E. N. (2021). VDAC modulation of cancer metabolism: Advances and therapeutic challenges. *Frontiers in Physiology*, *12*, 742839. https://doi.org/10.3389/FPHYS.2021.742839/BIBTEX

Hirata, Y., Cai, R., Volchuk, A., Matsuzawa, A., Grinstein, S., Correspondence, S. A. F., Steinberg, B. E., Saito, Y., & Freeman, S. A. (2023). Lipid peroxidation increases membrane tension, Piezo1 gating, and cation permeability to execute ferroptosis. *Current Biology*, *33*. https://doi.org/10.1016/j.cub.2023.02.060

Hjalgrim, H., Edgren, G., Rostgaard, K., Reilly, M., Tran, T. N., Titlestad, K. E., Shanwell, A., Jersild, C., Adami, J., Wikman, A., Gridley, G., Wideroff, L., Nyrén, O., & Melbye, M. (2007). Cancer incidence in blood transfusion recipients. *JNCI: Journal of the National Cancer Institute*, *99*(24), 1864–1874. https://doi.org/10.1093/JNCI/DJM248

Hole, P. S., Zabkiewicz, J., Munje, C., Newton, Z., Pearn, L., White, P., Marquez, N., Hills, R. K., Burnett, A. K., Tonks, A., & Darley, R. L. (2013). Overproduction of NOX-derived ROS in AML promotes proliferation and is associated with defective oxidative stress signaling. *Blood*, *122*(19), 3322–3330. https://doi.org/10.1182/BLOOD-2013-04-491944

Hopkins, B. D., Hodakoski, C., Barrows, D., Mense, S. M., & Parsons, R. E. (2014). PTEN function, the long and the short of it. *Trends in Biochemical Sciences*, *39*(4), 183. https://doi.org/10.1016/J.TIBS.2014.02.006

Hou, W., Xie, Y., Song, X., Sun, X., Lotze, M. T., Zeh, H. J., Kang, R., & Tang, D. (2016). Autophagy promotes ferroptosis by degradation of ferritin. *Autophagy*, *12*(8), 1425–1428. https://doi.org/10.1080/15548627.2016.1187366

Hume, D. A. (2006). The mononuclear phagocyte system. *Current Opinion in Immunology*, *18*(1), 49–53. https://doi.org/10.1016/J.COI.2005.11.008

Ibrahim, O., & O'Sullivan, J. (2020). Iron chelators in cancer therapy. *BioMetals*, *33*(4–5), 201–215. https://doi.org/10.1007/S10534-020-00243-3/TABLES/3

Jabbour, E., & Kantarjian, H. (2018). Chronic myeloid leukemia: 2018 update on diagnosis, therapy and monitoring. *American Journal of Hematology*, *93*(3), 442–459. https://doi.org/10.1002/AJH.25011

Jian, N., Dowle, M., Horniblow, R. D., Tselepis, C., & Palmer, R. E. (2016). Morphology of the ferritin iron core by aberration corrected scanning transmission electron microscopy. *Nanotechnology*, *27*(46), 46LT02. https://doi.org/10.1088/0957-4484/27/46/46LT02

Jiang, L., Kon, N., Li, T., Wang, S. J., Su, T., Hibshoosh, H., Baer, R., & Gu, W. (2015). Ferroptosis as a p53-mediated activity during tumour suppression. *Nature 2015 520:7545*, *520*(7545), 57–62. https://doi.org/10.1038/nature14344

Johnson, D. C., Dean, D. R., Smith, A. D., & Johnson, M. K. (2005). Structure, function, and formation of biological iron-sulfur clusters. *Annual Review of Biochemistry*, *74*, 247–281. https://doi.org/10.1146/ANNUREV.BIOCHEM.74.082803.133518

Kagan, V. E., Mao, G., Qu, F., Angeli, J. P. F., Doll, S., Croix, C. S., Dar, H. H., Liu, B., Tyurin, V. A., Ritov, V. B., Kapralov, A. A., Amoscato, A. A., Jiang, J., Anthonymuthu, T., Mohammadyani, D., Yang, Q., Proneth, B., Klein-Seetharaman, J., Watkins, S., … Baylr, H. (2016). Oxidized arachidonic and adrenic PEs navigate cells to ferroptosis. *Nature Chemical Biology*, *13*(1), 81–90. https://doi.org/10.1038/nchembio.2238

Kaphan, E., Laurin, D., Lafeuillade, B., Drillat, P., & Park, S. (2020). Impact of transfusion on survival in patients with myelodysplastic syndromes: Current knowledge, new insights and transfusion clinical practice. *Blood Reviews*, *41*, 100649. https://doi.org/10.1016/J.BLRE.2019.100649

Kawabata, H. (2019). Transferrin and transferrin receptors update. *Free Radical Biology and Medicine*, *133*, 46–54. https://doi.org/10.1016/J.FREERADBIOMED.2018.06.037

Kawabata, H., Nakamaki, T., Ikonomi, P., Smith, R. D., Germain, R. S., & Phillip Koeffler, H. (2001). Expression of transferrin receptor 2 in normal and neoplastic hematopoietic cells. *Blood*, *98*(9), 2714–2719. https://doi.org/10.1182/BLOOD.V98.9.2714

Kennedy, A. E., Kamdar, K. Y., Lupo, P. J., Okcu, M. F., Scheurer, M. E., Baum, M. K., & Dorak, M. T. (2014). Examination of HFE associations with childhood leukemia risk and extension to other iron regulatory genes. *Leukemia Research*, *38*(9), 1055–1060. https://doi.org/10.1016/J.LEUKRES.2014.06.016

Kim, E., Annibal, A., Lee, Y., Park, H. E. H., Ham, S., Jeong, D. E., Kim, Y., Park, S., Kwon, S., Jung, Y., Park, J. S., Kim, S. S., Antebi, A., & Lee, S. J. V. (2023). Mitochondrial aconitase suppresses immunity by modulating oxaloacetate and the mitochondrial unfolded protein response. *Nature Communications*, *14*(1), 1–16. https://doi.org/10.1038/s41467-023-39393-6

Kim, J. L., Lee, D. H., Na, Y. J., Kim, B. R., Jeong, Y. A., Lee, S. Il, Kang, S., Joung, S. Y., Lee, S. Y., Oh, S. C., & Min, B. W. (2016). Iron chelator-induced apoptosis via the ER stress pathway in gastric cancer cells. *Tumor Biology*, *37*(7), 9709–9719. https://doi.org/10.1007/S13277-016-4878-4/FIGURES/5

Kinowaki, Y., Kurata, M., Ishibashi, S., Ikeda, M., Tatsuzawa, A., Yamamoto, M., Miura, O., Kitagawa, M., & Yamamoto, K. (2018). Glutathione peroxidase 4

overexpression inhibits ROS-induced cell death in diffuse large B-cell lymphoma. *Laboratory Investigation*, *98*(5), 609–619. https://doi.org/10.1038/S41374-017-0008-1

Kirtonia, A., Sethi, G., & Garg, M. (2020). The multifaceted role of reactive oxygen species in tumorigenesis. *Cellular and Molecular Life Sciences*, *77*(22), 4459–4483. https://doi.org/10.1007/S00018-020-03536-5/FIGURES/9

Koc, M., Nad'ová, Z., Truksa, J., Ehrlichová, M., & Kovář, J. (2005). Iron deprivation induces apoptosis via mitochondrial changes related to Bax translocation. *Apoptosis*, *10*(2), 381–393. https://doi.org/10.1007/S10495-005-0812-8/METRICS

Kraml, P. J., Klein, R. L., Huang, Y., Nareika, A., & Lopes-Virella, M. F. (2005). Iron loading increases cholesterol accumulation and macrophage scavenger receptor I expression in THP-1 mononuclear phagocytes. *Metabolism*, *54*(4), 453–459. https://doi.org/10.1016/J.METABOL.2004.10.012

Kumada, H., Itoh, M., & Tohda, S. (2024). Effect of ferroptosis inducers and inhibitors on cell proliferation in acute leukemia. *Anticancer Research*, *44*(3), 1003–1010. https://doi.org/10.21873/ANTICANRES.16895

Leardi, A., Caraglia, M., Selleri, C., Pepe, S., Pizzi, C., Notaro, R., Fabbrocini, A., De Lorenzo, S., Musico, M., Abbruzzese, A., Bianco, A. R., & Tagliaferri, P. (2001). Desferioxamine increases iron depletion and apoptosis induced by ara-C of human myeloid leukaemic cells. *British Journal of Haematology*, *102*(3), 746–752. https://doi.org/10.1046/J.1365-2141.1998.00834.X

Lee, D. Y., Yun, S. H., Lee, S. Y., Lee, J., Mariano, E., Joo, S. T., Choi, I., Choi, J. S., Kim, G. D., Lee, J., Choi, S. H., & Hur, S. J. (2023). Analysis of commercial fetal bovine serum (FBS) and its substitutes in the development of cultured meat. *Food Research International*, *174*, 113617. https://doi.org/10.1016/J.FOODRES.2023.113617

Lenaz, G. (2012). Mitochondria and reactive oxygen species. Which role in physiology and pathology? *Advances in Experimental Medicine and Biology*, *942*, 93–136. https://doi.org/10.1007/978-94-007-2869-1_5/FIGURES/6_5

Levrero, M., De Laurenzi, V., Costanzo, A., Sabatini, S., Gong, J., Wang, J. Y. J., & Melino, G. (2000). The p53/p63/p73 family of transcription factors: Overlapping and distinct functions. *Journal of Cell Science*, *113*(10), 1661–1670. https://doi.org/10.1242/JCS.113.10.1661

Li, J., Cao, F., Yin, H. liang, Huang, Z. jian, Lin, Z. tao, Mao, N., Sun, B., & Wang, G. (2020). Ferroptosis: past, present and future. *Cell Death & Disease*, *11*(2), 1–13. https://doi.org/10.1038/s41419-020-2298-2

Liu, Q., Wang, M., Hu, Y., Xing, H., Chen, X., Zhang, Y., & Zhu, P. (2014). Significance of CD71 expression by flow cytometry in diagnosis of acute leukemia. *Leukemia and Lymphoma*, *55*(4), 892–898. https://doi.org/10.3109/10428194.2013.819100/SUPPL_FILE/DISCLOSURE.ZIP

Liu, Y., & Zhu, Z. (2022). Study on the mitochondrial autophagy pathway of apoptosis induced by deferoxamine in the leukemia cell line HL-60. *Iranian Journal of Pediatrics*, *32*(4). https://doi.org/10.5812/IJP-119937

Lizier, M., Anselmo, A., Mantero, S., Ficara, F., Paulis, M., Vezzoni, P., Lucchini, F., & Pacchiana, G. (2016). Fusion between cancer cells and macrophages occurs in a murine model of spontaneous Neu+ breast cancer without increasing its metastatic potential. *Oncotarget*, *7*(38), 60793. https://doi.org/10.18632/ONCOTARGET.11508

Lu, S. C. (2009). Regulation of glutathione synthesis. *Molecular Aspects of Medicine*, *30*(1–2), 42–59. https://doi.org/10.1016/J.MAM.2008.05.005

Lu, S. C. (2013). Glutathione synthesis. *Biochimica et Biophysica Acta (BBA) - General Subjects*, *1830*(5), 3143–3153. https://doi.org/10.1016/J.BBAGEN.2012.09.008

Ludin, A., Gur-Cohen, S., Golan, K., Kaufmann, K. B., Itkin, T., Medaglia, C., Lu, X. J., Ledergor, G., Kollet, O., & Lapidot, T. (2014). Reactive oxygen species regulate hematopoietic stem cell self-renewal, migration and development, as well as their bone marrow microenvironment. *Antioxidants & Redox Signaling*, *21*(11), 1605–1619. https://doi.org/10.1089/ARS.2014.5941

Ma, Y., Zhou, T., Kong, X., & C. Hider, R. (2012). Chelating agents for the treatment of systemic iron overload. *Current Medicinal Chemistry*, *19*(17), 2816–2827. https://doi.org/10.2174/092986712800609724

Maldonado, E. N. (2017). VDAC-tubulin, an anti-Warburg pro-oxidant switch. *Frontiers in Oncology*, *7*, 4. https://doi.org/10.3389/FONC.2017.00004/BIBTEX

Maldonado, E. N., Sheldon, K. L., Dehart, D. N., Patnaik, J., Manevich, Y., Townsend, D. M., Bezrukov, S. M., Rostovtseva, T. K., & Lemasters, J. J. (2013). Voltage-dependent anion channels modulate mitochondrial metabolism in cancer cells: Regulation by free tubulin and erastin. *Journal of Biological Chemistry*, *288*(17), 11920–11929.

https://doi.org/10.1074/JBC.M112.433847/ATTACHMENT/E017059D-831E-488C-A081-E8EF31EA608A/MMC1.ZIP

Maniecki, M. B., Møller, H. J., Moestrup, S. K., & Møller, B. K. (2006). CD163 positive subsets of blood dendritic cells: The scavenging macrophage receptors CD163 and CD91 are coexpressed on human dendritic cells and monocytes. *Immunobiology*, *211*(6–8), 407–417. https://doi.org/10.1016/J.IMBIO.2006.05.019

Marei, H. E., Althani, A., Afifi, N., Hasan, A., Caceci, T., Pozzoli, G., Morrione, A., Giordano, A., & Cenciarelli, C. (2021). p53 signaling in cancer progression and therapy. *Cancer Cell International*, *21*(1), 1–15. https://doi.org/10.1186/S12935-021-02396-8/FIGURES/4

Masarova, L., Bose, P., Pemmaraju, N., Daver, N., Zhou, L., Pierce, S., Kantarjian, H., Estrov, Z., & Verstovsek, S. (2021). Clinical significance of bone marrow blast percentage in patients with myelofibrosis and the effect of ruxolitinib therapy. *Clinical Lymphoma, Myeloma & Leukemia*, *21*(5), 318. https://doi.org/10.1016/J.CLML.2020.12.024

Mashima, R., & Okuyama, T. (2015). The role of lipoxygenases in pathophysiology; new insights and future perspectives. *Redox Biology*, *6*, 297. https://doi.org/10.1016/J.REDOX.2015.08.006

Mazure, N. M. (2017). VDAC in cancer. *Biochimica et Biophysica Acta (BBA) - Bioenergetics*, *1858*(8), 665–673. https://doi.org/10.1016/J.BBABIO.2017.03.002

Michel, H., Behr, J., Harrenga, A., & Kannt, A. (1998). Cytochrome C oxidase: Structure and spectroscopy. *Annual Review of Biophysics and Biomolecular Structure*, *27*, 329–356. https://doi.org/10.1146/ANNUREV.BIOPHYS.27.1.329

Moloney, J. N., & Cotter, T. G. (2018). ROS signalling in the biology of cancer. *Seminars in Cell & Developmental Biology*, *80*, 50–64. https://doi.org/10.1016/J.SEMCDB.2017.05.023

Montesano, R., & Hall, J. (2001). Environmental causes of human cancers. *European Journal of Cancer*, *37*(SUPPL. 8), 67–87. https://doi.org/10.1016/S0959-8049(01)00266-0

Moreaux, J., Kassambara, A., Hose, D., & Klein, B. (2012). STEAP1 is overexpressed in cancers: A promising therapeutic target. *Biochemical and Biophysical Research Communications*, *429*(3–4), 148–155. https://doi.org/10.1016/J.BBRC.2012.10.123

Nebert, D. W., & Russell, D. W. (2002). Clinical importance of the cytochromes P450. *Lancet*, *360*(9340), 1155–1162. https://doi.org/10.1016/S0140-6736(02)11203-7

Neumannova, V., Richardson, D. R., Kriegerbeckova, K., & Kovar, J. (1995). Growth of human tumor cell lines in transferrin-free, low-iron medium. *In Vitro Cellular & Developmental Biology - Animal*, *31*(8), 625–632. https://doi.org/10.1007/BF02634316/METRICS

Pande, A., Dorwal, P., Jain, D., Tyagi, N., Mehra, S., Sachdev, R., & Raina, V. (2016). Expression of CD71 by flow cytometry in acute leukemias: More often seen in acute myeloid leukemia. *Indian Journal of Pathology and Microbiology*, *59*(3), 310–313. https://doi.org/10.4103/0377-4929.188145

Pandur, E., Tamási, K., Pap, R., Jánosa, G., & Sipos, K. (2022). Modulatory effects of fractalkine on inflammatory response and iron metabolism of lipopolysaccharide and lipoteichoic acid-activated THP-1 macrophages. *International Journal of Molecular Sciences*, *23*(5), 2629. https://doi.org/10.3390/IJMS23052629/S1

Pavlova, N. N., Zhu, J., & Thompson, C. B. (2022). The hallmarks of cancer metabolism: Still emerging. *Cell Metabolism*, *34*(3), 355–377. https://doi.org/10.1016/J.CMET.2022.01.007

Plays, M., Müller, S., & Rodriguez, R. (2021). Chemistry and biology of ferritin. *Metallomics*, *13*(5), 21. https://doi.org/10.1093/MTOMCS/MFAB021

Präbst, K., Engelhardt, H., Ringgeler, S., & Hübner, H. (2017). Basic colorimetric proliferation assays: MTT, WST, and resazurin. *Methods in Molecular Biology*, *1601*, 1–17. https://doi.org/10.1007/978-1-4939-6960-9_1/FIGURES/6

Prior, I. A., Hood, F. E., & Hartley, J. L. (2020). The frequency of ras mutations in cancer. *Cancer Research*, *80*(14), 2669–2974. https://doi.org/10.1158/0008-5472.CAN-19-3682/653980/AM/THE-FREQUENCY-OF-RAS-MUTATIONS-IN-CANCERRAS-CANCER

Propper, R. D., Cooper, B., Rufo, R. R., Nienhuis, A. W., Anderson, W. F., Bunn, H. F., Rosenthal, A., & Nathan, D. G. (1977). Continuous subcutaneous administration of deferoxamine in patients with iron overload. *New England Journal of Medicine*, *297*(8), 418–423. https://doi.org/10.1056/NEJM197708252970804

Puig, S., Ramos-Alonso, L., Romero, A. M., & Martínez-Pastor, M. T. (2017). The elemental role of iron in DNA synthesis and repair. *Metallomics*, *9*(11), 1483–1500. https://doi.org/10.1039/C7MT00116A

Qingmei, J., Jinping, L., Jie, G., & Junzhu, W. (2010). Effects of DMT-1 in LDL oxidation mediated by cells. *Europe PMC,* 563-565. https://europepmc.org/article/cba/644511

Rahman, I., Kode, A., & Biswas, S. K. (2007). Assay for quantitative determination of glutathione and glutathione disulfide levels using enzymatic recycling method. *Nature Protocols*, *1*(6), 3159–3165. https://doi.org/10.1038/nprot.2006.378

Rassool, F. V., Gaymes, T. J., Omidvar, N., Brady, N., Beurlet, S., Pla, M., Reboul, M., Lea, N., Chomienne, C., Thomas, N. S. B., Mufti, G. J., & Padua, R. A. (2007). Reactive oxygen species, DNA damage, and error-prone repair: A model for genomic instability with progression in myeloid leukemia? *Cancer Research*, *67*(18), 8762–8771. https://doi.org/10.1158/0008-5472.CAN-06-4807

Reddy, P. V., Puri, R. V., Khera, A., & Tyagi, A. K. (2012). Iron storage proteins are essential for the survival and pathogenesis of Mycobacterium tuberculosis in THP-1 macrophages and the guinea pig model of infection. *Journal of Bacteriology*, *194*(3), 567–575. https://doi.org/10.1128/JB.05553-11/SUPPL_FILE/SUPPLEMENTALMATERIAL.DOC

Reedy, C. J., & Gibney, B. R. (2004). Heme protein assemblies. *Chemical Reviews*, *104*(2), 617–649. https://doi.org/10.1021/CR0206115/SUPPL_FILE/CR0206115_S.PDF

Risko, P., Buchal, R., Kraml, P., Pláteník, J., & Potocková, J. (2015). THP-I cells as a model of human monocytes in iron-loading conditions. *Atherosclerosis*, *241*(1), e80. https://doi.org/10.1016/J.ATHEROSCLEROSIS.2015.04.280

Rose-Inman, H., & Kuehl, D. (2017). Acute leukemia. *Hematology/Oncology Clinics of North America*, *31*(6), 1011–1028. https://doi.org/10.1016/j.hoc.2017.08.006

Saliba, A. N., Harb, A. R., & Taher, A. T. (2015). Iron chelation therapy in transfusion-dependent thalassemia patients: Current strategies and future directions. *Journal of Blood Medicine*, *6*, 197–209. https://doi.org/10.2147/JBM.S72463

Salk, J. J., Fox, E. J., & Loeb, L. A. (2010). Mutational heterogeneity in human cancers: Origin and consequences. *Annual Review of Pathology: Mechanisms of Disease*, *5*, 51–75. https://doi.org/10.1146/ANNUREV-PATHOL-121808-102113

Sato, M., Kusumi, R., Hamashima, S., Kobayashi, S., Sasaki, S., Komiyama, Y., Izumikawa, T., Conrad, M., Bannai, S., & Sato, H. (2018). The ferroptosis inducer erastin irreversibly inhibits system x_C^- and synergizes with cisplatin to increase cisplatin's cytotoxicity in cancer cells. *Scientific Reports*, *8*(1), 1–9. https://doi.org/10.1038/s41598-018-19213-4

Schär, P. (2001). Spontaneous DNA damage, genome instability, and cancer - When DNA replication escapes control. *Cell*, *104*(3), 329–332. https://doi.org/10.1016/S0092-8674(01)00220-3

*SEER*Explorer: An interactive website for SEER cancer statistics*. (2023). National Cancer Institute. https://seer.cancer.gov/statistics-network/explorer/

Seiler, A., Schneider, M., Förster, H., Roth, S., Wirth, E. K., Culmsee, C., Plesnila, N., Kremmer, E., Rådmark, O., Wurst, W., Bornkamm, G. W., Schweizer, U., & Conrad, M. (2008). Glutathione peroxidase 4 senses and translates oxidative stress into 12/15-lipoxygenase dependent- and AIF-mediated cell death. *Cell Metabolism*, *8*(3), 237–248. https://doi.org/10.1016/j.cmet.2008.07.005

Semenza, G. L. (2001). HIF-1 and mechanisms of hypoxia sensing. *Current Opinion in Cell Biology*, *13*(2), 167–171. https://doi.org/10.1016/S0955-0674(00)00194-0

Seo, G. S., Lee, S. H., Choi, S. C., Choi, E. Y., Oh, H. M., Choi, E. J., Park, D. S., Kim, S. W., Kim, T. H., Nah, Y. H., Kim, S., Kim, S. H., You, S. H., & Jun, C. D. (2006). Iron chelator induces THP-1 cell differentiation potentially by modulating intracellular glutathione levels. *Free Radical Biology and Medicine*, *40*(9), 1502–1512. https://doi.org/10.1016/J.FREERADBIOMED.2005.12.020

Shah, R., Shchepinov, M. S., & Pratt, D. A. (2018). Resolving the role of lipoxygenases in the initiation and execution of ferroptosis. *ACS Central Science*, *4*(3), 387–396. https://doi.org/10.1021/ACSCENTSCI.7B00589/ASSET/IMAGES/LARGE/OC-2017-00589W_0006.JPEG

Shapira, S., Raanani, P., Samara, A., Nagler, A., Lubin, I., Arber, N., & Granot, G. (2019). Deferasirox selectively induces cell death in the clinically relevant population of leukemic CD34+ CD38- cells through iron chelation, induction of ROS, and inhibition of HIF1α expression. *Experimental Hematology*, *70*, 55-69. https://doi.org/10.1016/j.exphem.2018.10.010

Sherr, C. J. (2004). Principles of tumor suppression. *Cell*, *116*(2), 235–246. https://doi.org/10.1016/S0092-8674(03)01075-4

Shimizu, S., Ide, T., Yanagida, T., & Tsujimoto, Y. (2000). Electrophysiological study of a novel large pore formed by Bax and the voltage-dependent anion channel that is permeable to cytochrome c. *Journal of Biological Chemistry*, *275*(16), 12321–12325. https://doi.org/10.1074/jbc.275.16.12321

Shimizu, S., Matsuoka, Y., Shinohara, Y., Yoneda, Y., & Tsujimoto, Y. (2001). Essential role of voltage-dependent anion channel in various forms of apoptosis in

mammalian cells. *Journal of Cell Biology*, *152*(2), 237–250. https://doi.org/10.1083/JCB.152.2.237

Singh, R., Lemire, J., Mailloux, R. J., & Appanna, V. D. (2008). A novel strategy involved anti-oxidative defense: The conversion of NADH into NADPH by a metabolic network. *PLOS ONE*, *3*(7), e2682. https://doi.org/10.1371/JOURNAL.PONE.0002682

Soeur, J., Eilstein, J., Léreaux, G., Jones, C., & Marrot, L. (2015). Skin resistance to oxidative stress induced by resveratrol: From Nrf2 activation to GSH biosynthesis. *Free Radical Biology and Medicine*, *78*, 213–223. https://doi.org/10.1016/J.FREERADBIOMED.2014.10.510

Stevens, R. G., Graubard, B. I., Micozzi, M. S., Neriishi, K., & Blumberg, B. S. (1994). Moderate elevation of body iron level and increased risk of cancer occurrence and death. *International Journal of Cancer*, *56*(3), 364–369. https://doi.org/10.1002/IJC.2910560312

Stockwell, B. R., Friedmann Angeli, J. P., Bayir, H., Bush, A. I., Conrad, M., Dixon, S. J., Fulda, S., Gascón, S., Hatzios, S. K., Kagan, V. E., Noel, K., Jiang, X., Linkermann, A., Murphy, M. E., Overholtzer, M., Oyagi, A., Pagnussat, G. C., Park, J., Ran, Q., … Zhang, D. D. (2017). Ferroptosis: A regulated cell death nexus linking metabolism, redox biology, and disease. *Cell*, *171*(2), 273–285. https://doi.org/10.1016/J.CELL.2017.09.021

Strober, W. (2015). Trypan blue exclusion test of cell viability. *Current Protocols in Immunology*, *111*(1), A3.B.1-A3.B.3. https://doi.org/10.1002/0471142735.IMA03BS111

Sugimoto, K., Toyoshima, H., Sakai, R., Miyagawa, K., Hagiwara, K., Ishikawa, F., Takaku, F., Yazaki, Y., & Hirai, H. (1992). Frequent mutations in the p53 gene in human myeloid leukemia cell lines. *Blood*, *79*(9), 2378–2383. https://doi.org/10.1182/BLOOD.V79.9.2378.2378

Sun, Y., Zheng, Y., Wang, C., & Liu, Y. (2018). Glutathione depletion induces ferroptosis, autophagy, and premature cell senescence in retinal pigment epithelial cells. *Cell Death & Disease*, *9*(7), 1–15. https://doi.org/10.1038/s41419-018-0794-4

Swerdlow, S. H., Campo, E., Harris, N. L., Jaffe, E. S., Pileri, S. A., Stein, H., Thiele, J., & Vardiman, J. W. (2008). *WHO Classification of Tumours of Haematopoietic and Lymphoid Tissues, 4th Ed*.

Tataranni, T., Agriesti, F., Mazzoccoli, C., Ruggieri, V., Scrima, R., Laurenzana, I., D'Auria, F., Falzetti, F., Di Ianni, M., Musto, P., Capitanio, N., & Piccoli, C. (2015). The iron chelator deferasirox affects redox signalling in haematopoietic stem/progenitor cells. *British Journal of Haematology*, *170*(2), 236–246. https://doi.org/10.1111/BJH.13381

Todd, R., & Munger, K. (2006). Oncogenes. *Encyclopedia of Life Sciences*. https://doi.org/10.1002/9780470015902.A0006006

Torti, S. V., Manz, D. H., Paul, B. T., Blanchette-Farra, N., & Torti, F. M. (2018). Iron and cancer. *Annual Review of Nutrition*, *38*, 97–125. https://doi.org/10.1146/ANNUREV-NUTR-082117-051732

Tsuchiya, S., Yamabe, M., Yamaguchi, Y., Kobayashi, Y., Konno, T., & Tada, K. (1980). Establishment and characterization of a human acute monocytic leukemia cell line (THP-1). *International Journal of Cancer*, *26*(2), 171–176. https://doi.org/10.1002/IJC.2910260208

Varotto, E., Munaretto, E., Stefanachi, F., Della Torre, F., & Buldini, B. (2022). Diagnostic challenges in acute monoblastic/monocytic leukemia in children. *Frontiers in Pediatrics*, *10*. https://doi.org/10.3389/FPED.2022.911093/BIBTEX

Vinchi, F., Hell, S., & Platzbecker, U. (2020). Controversies on the consequences of iron overload and chelation in MDS. *HemaSphere*, *4*(3), e357. https://doi.org/10.1097/HS9.0000000000000357

Visvader, J. E. (2011). Cells of origin in cancer. *Nature*, *469*(7330), 314–322. https://doi.org/10.1038/nature09781

von Krusenstiern, A. N., Robson, R. N., Qian, N., Qiu, B., Hu, F., Reznik, E., Smith, N., Zandkarimi, F., Estes, V. M., Dupont, M., Hirschhorn, T., Shchepinov, M. S., Min, W., Woerpel, K. A., & Stockwell, B. R. (2023). Identification of essential sites of lipid peroxidation in ferroptosis. *Nature Chemical Biology*, *19*(6), 719–730. https://doi.org/10.1038/s41589-022-01249-3

Wang, F., Lv, H., Zhao, B., Zhou, L., Wang, S., Luo, J., Liu, J., & Shang, P. (2019). Iron and leukemia: New insights for future treatments. *Journal of Experimental & Clinical Cancer Research: CR*, *38*. https://doi.org/10.1186/S13046-019-1397-3

Weber, S., Parmon, A., Kurrle, N., Schnütgen, F., & Serve, H. (2021). The clinical significance of iron overload and iron metabolism in myelodysplastic syndrome and acute myeloid leukemia. *Frontiers in Immunology*, *11*. https://doi.org/10.3389/FIMMU.2020.627662/BIBTEX

Wessling-Resnick, M. (2010). Iron homeostasis and the inflammatory response. *Annual Reviews of Nutrition*. https://doi.org/10.1146/ANNUREV.NUTR.012809.104804

Wu, T., Sempos, C. T., Freudenheim, J. L., Muti, P., & Smit, E. (2004). Serum iron, copper and zinc concentrations and risk of cancer mortality in US adults. *Annals of Epidemiology*, *14*(3), 195–201. https://doi.org/10.1016/S1047-2797(03)00119-4

Wu, W., Geng, Z., Bai, H., Liu, T., & Zhang, B. (2021). Ammonium ferric citrate induced ferroptosis in non-small-cell lung carcinoma through the inhibition of GPX4-GSS/GSR-GGT axis activity. *International Journal of Medical Sciences*, *18*(8), 1899. https://doi.org/10.7150/IJMS.54860

Xia, Y., Liu, Y., Yang, C., Simeone, D. M., Sun, T. T., DeGraff, D. J., Tang, M. shong, Zhang, Y., & Wu, X. R. (2021). Dominant role of CDKN2B/p15INK4B of 9p21.3 tumor suppressor hub in inhibition of cell-cycle and glycolysis. *Nature Communications*, *12*(1), 1–15. https://doi.org/10.1038/s41467-021-22327-5

Xie, Y., Hou, W., Song, X., Yu, Y., Huang, J., Sun, X., Kang, R., & Tang, D. (2016). Ferroptosis: Process and function. *Cell Death & Differentiation*, *23*(3), 369–379. https://doi.org/10.1038/cdd.2015.158

Xu, W., Barrientos, T., & Andrews, N. C. (2013). Iron and copper in mitochondrial diseases. *Cell Metabolism*, *17*, 319–328. https://doi.org/10.1016/j.cmet.2013.02.004

Xue, Y., Zhang, G., Zhou, S., Wang, S., Lv, H., Zhou, L., & Shang, P. (2021). Iron chelator induces apoptosis in osteosarcoma cells by disrupting intracellular iron homeostasis and activating the MAPK pathway. *International Journal of Molecular Sciences, 22*(13), 7168. https://doi.org/10.3390/IJMS22137168

Yalcintepe, L., & Halis, E. (2016). Modulation of iron metabolism by iron chelation regulates intracellular calcium and increases sensitivity to doxorubicin. *Biomolecules and Biomedicine*, *16*(1), 14–20. https://doi.org/10.17305/bjbms.2016.576

Yan, H. fa, Zou, T., Tuo, Q. zhang, Xu, S., Li, H., Belaidi, A. A., & Lei, P. (2021). Ferroptosis: mechanisms and links with diseases. *Signal Transduction and Targeted Therapy*, *6*(1), 1–16. https://doi.org/10.1038/s41392-020-00428-9

Yang, F., Wu, Z., Dai, D., Zhang, L., Zhang, X., Zhang, X., & Xu, Y. (2021). The iron chelator deferoxamine decreases myeloma cell survival. *Journal of International Medical Research*, *49*(1).

https://doi.org/10.1177/0300060520987396/ASSET/IMAGES/LARGE/10.1177_0300060520987396-FIG6.JPEG

Yang, W. S., & Stockwell, B. R. (2016). Ferroptosis: Death by lipid peroxidation. *Trends in Cell Biology*, *26*(3), 165–176. https://doi.org/10.1016/j.tcb.2015.10.014

Yang, Y., Xu, Y., Su, A., Yang, D., & Zhang, X. (2018). Effects of deferoxamine on leukemia in vitro and its related mechanism. *Medical Science Monitor: International Medical Journal of Experimental and Clinical Research*, *24*, 6735. https://doi.org/10.12659/MSM.910325

Ye, F., Chai, W., Xie, M., Yang, M., Yu, Y., Cao, L., & Yang, L. (2019). HMGB1 regulates erastin-induced ferroptosis via RAS-JNK/p38 signaling in HL-60/NRASQ61L cells. *American Journal of Cancer Research*, *9*(4), 730. /pmc/articles/PMC6511643/

Yoo, J. H., Maeng, H. Y., Sun, Y. K., Kim, Y. A., Park, D. W., Tae, S. P., Seung, T. L., & Choi, J. R. (2009). Oxidative status in iron-deficiency anemia. *Journal of Clinical Laboratory Analysis*, *23*(5), 319–323. https://doi.org/10.1002/JCLA.20335

Yousefzadeh, M., Henpita, C., Vyas, R., Soto-Palma, C., Robbins, P., & Niedernhofer, L. (2021). DNA damage—how and why we age? *ELife*, *10*, 1–17. https://doi.org/10.7554/ELIFE.62852

Yu, Y., Xie, Y., Cao, L., Yang, L., Yang, M., Lotze, M. T., Zeh, H. J., Kang, R., & Tang, D. (2015). The ferroptosis inducer erastin enhances sensitivity of acute myeloid leukemia cells to chemotherapeutic agents. *Molecular & Cellular Oncology*, *2*(4). https://doi.org/10.1080/23723556.2015.1054549

Zhang, C., & Zhang, F. (2015). Iron homeostasis and tumorigenesis: Molecular mechanisms and therapeutic opportunities. *Protein & Cell*, *6*(2), 88–100. https://doi.org/10.1007/S13238-014-0119-Z

Zhang, J., Hu, W., Ding, C., Yao, G., Zhao, H., & Wu, S. (2019). Deferoxamine inhibits iron-uptake stimulated osteoclast differentiation by suppressing electron transport chain and MAPKs signaling. *Toxicology Letters*, *313*, 50–59. https://doi.org/10.1016/J.TOXLET.2019.06.007

Zhang, Y., Fan, B. Y., Pang, Y. L., Shen, W. Y., Wang, X., Zhao, C. X., Li, W. X., Liu, C., Kong, X. H., Ning, G. Z., Feng, S. Q., & Yao, X. (2020). Neuroprotective effect of deferoxamine on erastininduced ferroptosis in primary cortical neurons. *Neural Regeneration Research*, *15*(8), 1539–1545. https://doi.org/10.4103/1673-5374.274344

Zhao, N., Zhang, A. S., Wortham, A. M., Jue, S., Knutson, M. D., & Enns, C. A. (2017). The Tumor Suppressor, P53, Decreases the Metal Transporter, ZIP14. *Nutrients*, *9*(12). https://doi.org/10.3390/NU9121335

Zhao, Y., Li, Y., Zhang, R., Wang, F., Wang, T., & Jiao, Y. (2020). The role of erastin in ferroptosis and its prospects in cancer therapy. *OncoTargets and Therapy*, *13*, 5429–5441. https://doi.org/10.2147/OTT.S254995

Zheng, Q. qing, Zhao, Y. shan, Guo, J., Zhao, S. da, Song, L. xi, Fei, C. ming, Zhang, Z., Li, X., & Chang, C. kang. (2017). Iron overload promotes erythroid apoptosis through regulating HIF-1a/ROS signaling pathway in patients with myelodysplastic syndrome. *Leukemia Research*, *58*, 55–62. https://doi.org/10.1016/J.LEUKRES.2017.04.005

Zolea, F., Biamonte, F., Candeloro, P., Di Sanzo, M., Cozzi, A., Di Vito, A., Quaresima, B., Lobello, N., Trecroci, F., Di Fabrizio, E., Levi, S., Cuda, G., & Costanzo, F. (2015). H ferritin silencing induces protein misfolding in K562 cells: A raman analysis. *Free Radical Biology and Medicine*, *89*, 614–623. https://doi.org/10.1016/J.FREERADBIOMED.2015.07.161

Appendix

Appendix A: Resazurin Assay Schematic

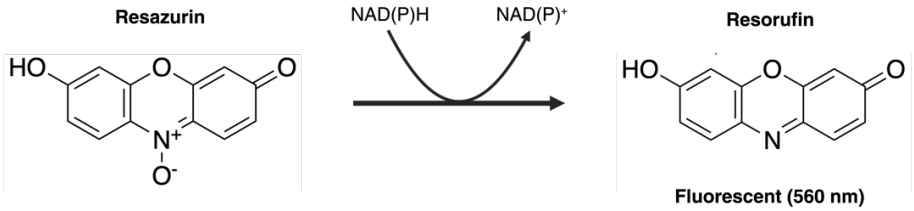

Figure 13. Mechanism of the resazurin metabolic assay.

Appendix B: DTNB Assay Schematic

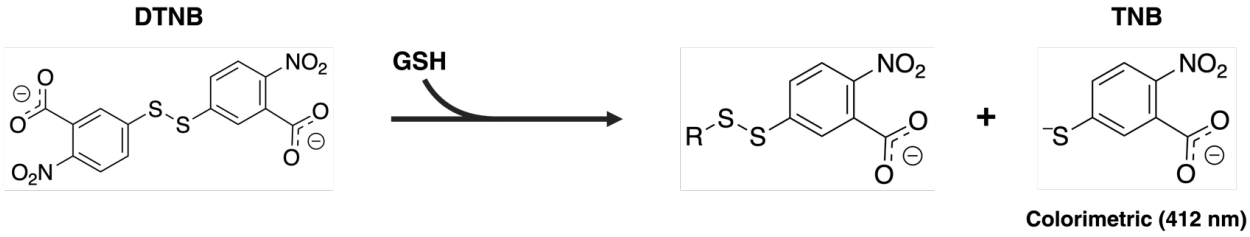

Figure 14. Mechanism of the DTNB assay.

Appendix C: Resazurin Assay Dose Response Curve

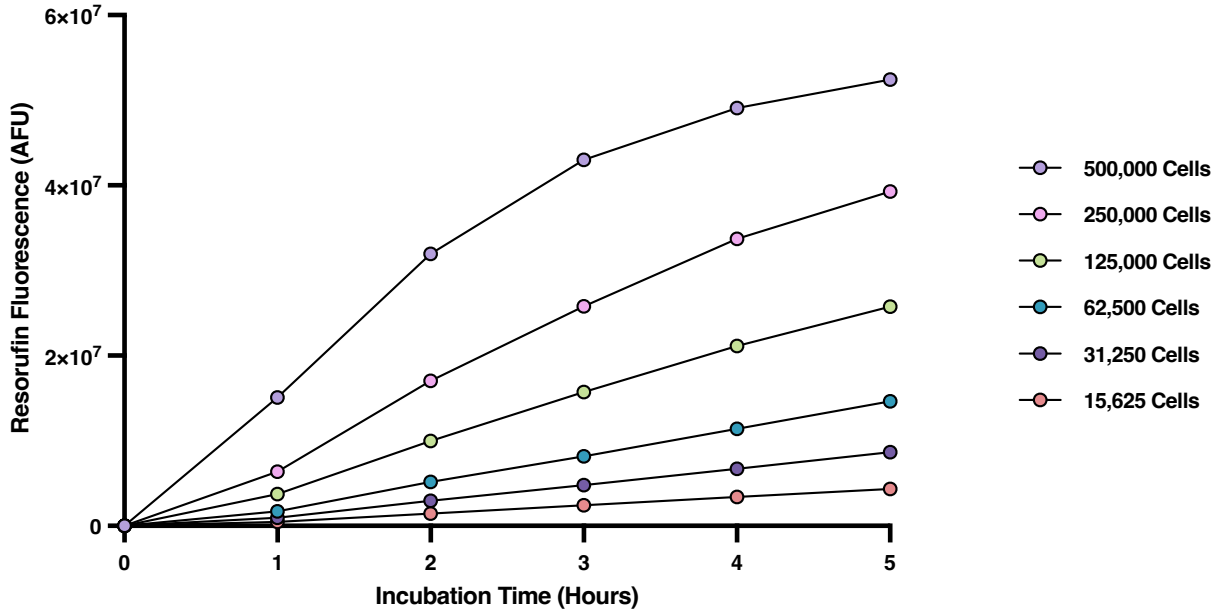

Figure 15. Dose-response curve of resorufin fluorescence at varying cell densities and incubation times. Aiming for a cell density and incubation time with a robust signal that fell within a linear section of the curve, these results suggested the ideal assay parameters with THP-1 cells were to measure 125,000 cells and to incubate for 3 hours.

Appendix D: Quantile-Quantile Plots of Normality

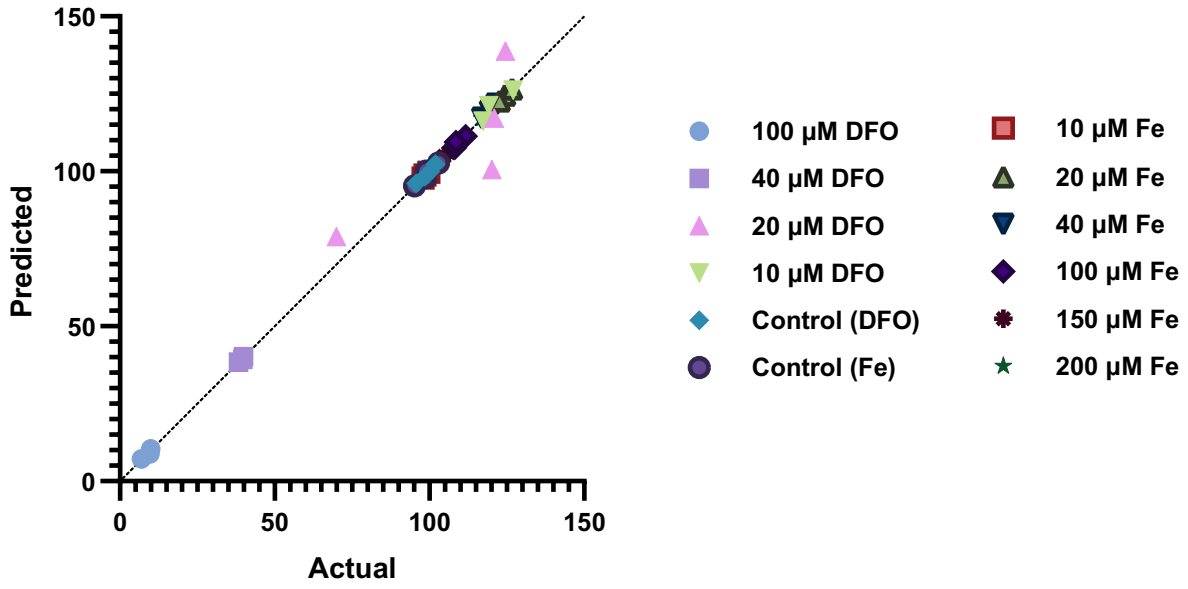

Figure 16. QQ plot of normality for THP-1 cell resazurin metabolic assay data shown in Figure 8. Fe, ferric citrate.

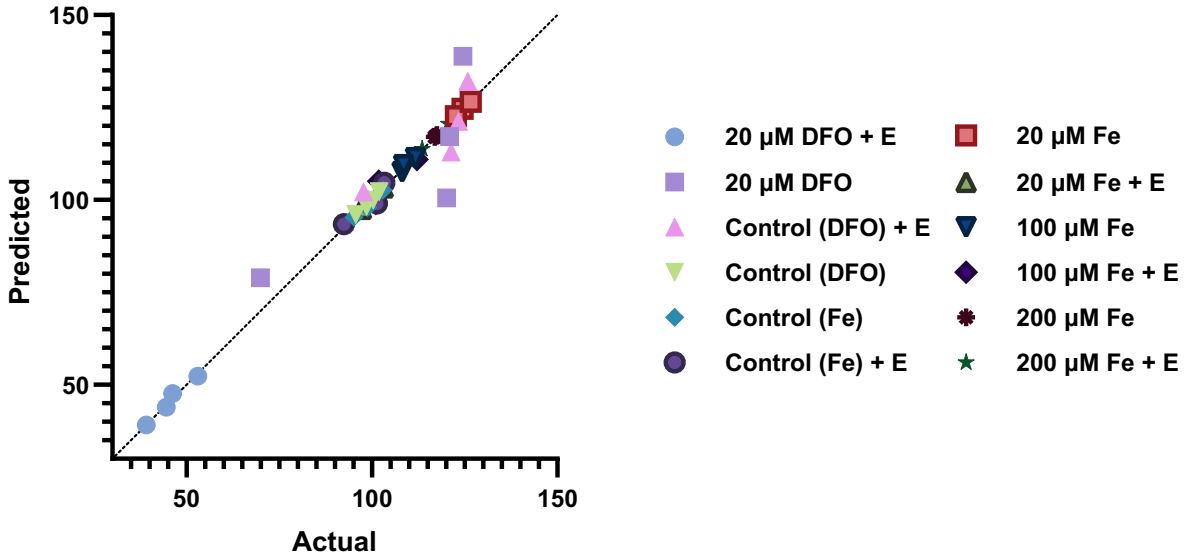

Figure 17. QQ plot of normality for THP-1 cell resazurin metabolic assay data shown in Figure 9. Fe, ferric citrate; E, 40 μM erastin.

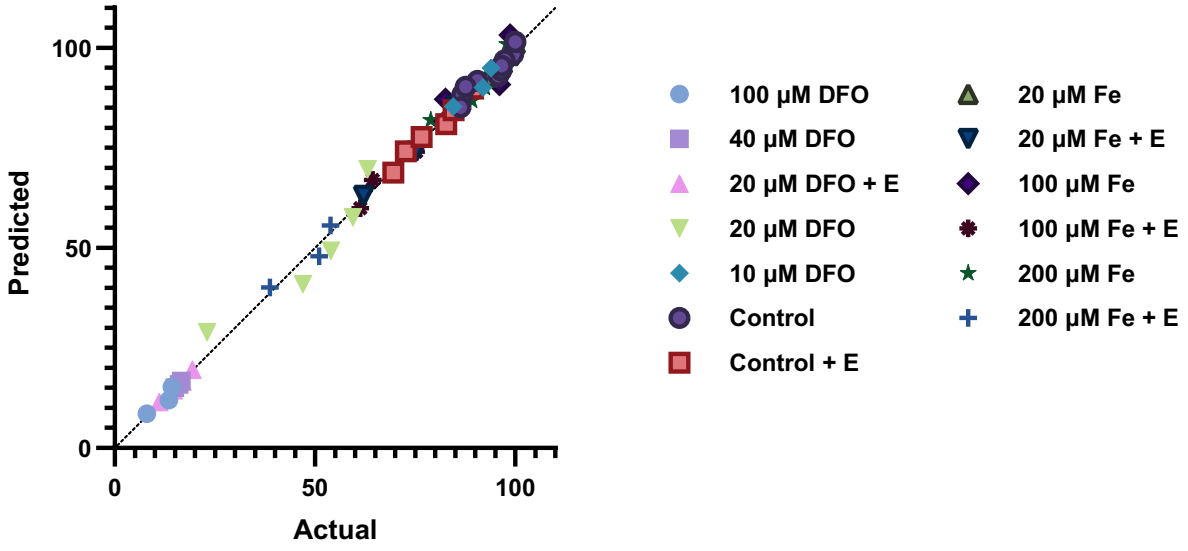

Figure 18. QQ plot of normality for trpan blue exclusion assay data shown in Figure 10. Fe, ferric citrate; E, 40 μM erastin

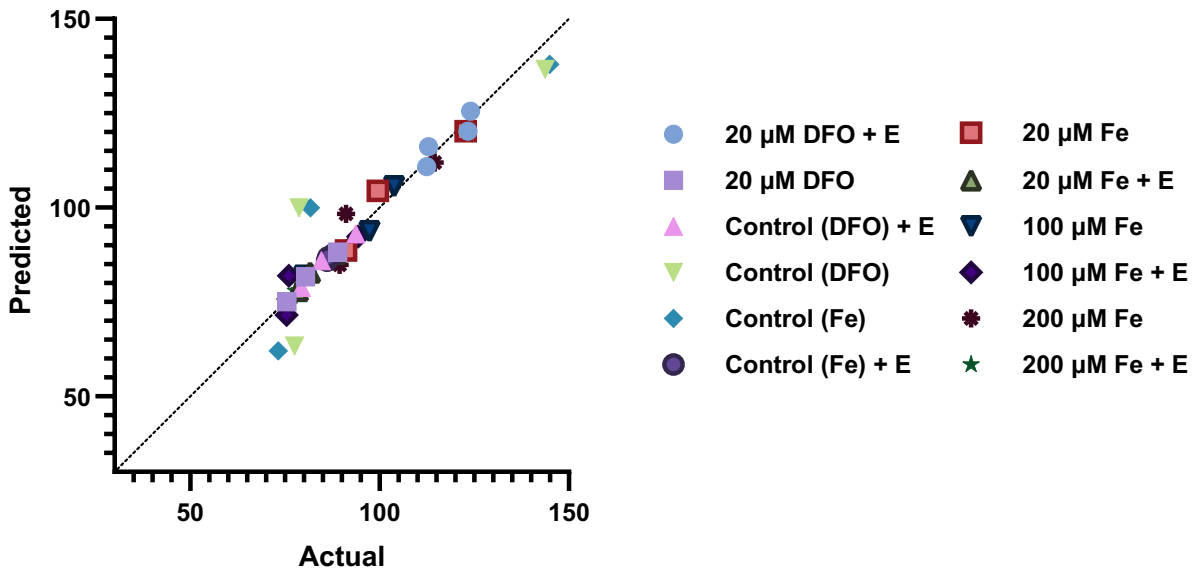

Figure 19. QQ plot of normality for DTNB assay data shown in Figure 12. Fe, ferric citrate; E, 40 μM erastin.